



universität  
wien

# DIPLOMARBEIT

Titel der Diplomarbeit

„A potential role for miR-31 in osteoblastic transition of  
vascular smooth muscle cells and cortisol-induced  
osteoporosis“

Verfasser

Maximilian Bönisch

angestrebter akademischer Grad

Magister der Naturwissenschaften (Mag.rer.nat.)

Wien, 2012

Studienkennzahl lt. Studienblatt:

A 441

Studienrichtung lt. Studienblatt:

Diplomstudium Genetik - Mikrobiologie (Stzw)

Betreuer:

Joachim Seipelt, PhD

# 1 Table of contents

2	Abstract .....	1
3	Introduction.....	1
3.1	Ageing and cellular senescence .....	1
3.1.1	Replicative senescence .....	3
3.1.2	Oncogene-induced senescence .....	4
3.1.3	Stress induced senescence in vitro .....	5
3.1.4	Linking cellular senescence with ageing .....	5
3.2	The ageing blood vessel .....	7
3.3	Cellular senescence in cardiovascular diseases .....	10
3.4	Calcification in vasculature and bone.....	12
3.4.1	Clinical relevance of atherosclerotic calcification.....	12
3.4.2	Bone calcification.....	13
3.4.3	Osteoblastic transition of VSMCs .....	14
3.5	MicroRNAs .....	15
3.5.1	MicroRNAs in ageing and cardiovascular diseases .....	17
3.5.2	miRNA-31 .....	18
3.6	Cortisol-induced osteoporosis .....	19
4	Aims.....	21
5	Materials and methods .....	22
5.1	Measurement of calcium-content and SYBR Green I staining .....	22
5.2	RNA-Isolation .....	24
5.3	cDNA-Synthesis .....	25
5.3.1	TaqMan .....	25
5.3.2	Dynamo .....	25
5.4	qPCR.....	26
5.4.1	TaqMan .....	26
5.4.2	Sensimix .....	26

5.5	cell culture .....	27
5.6	Alizarin Red S staining.....	28
5.7	Calcification assay (high $\text{Ca}^{2+}/\text{P}_i$ ).....	28
5.8	Calcification assay (low $\text{Ca}^{2+}/\text{P}_i$ ) – 1 <sup>st</sup> donor.....	29
5.9	Calcification assay (low $\text{Ca}^{2+}/\text{P}_i$ ) – 2 <sup>nd</sup> donor.....	31
5.10	Long-term hydrocortisone treatment .....	32
5.11	Luciferase reporter plasmid .....	33
5.11.1	DNA ladders.....	33
5.11.2	PCR .....	34
5.11.3	Addition of 3' A-overhangs .....	35
5.11.4	Blue/White screening .....	35
5.11.5	Ligation .....	35
5.11.6	Dephosphorylation .....	36
5.11.7	Chemical transformation .....	36
5.11.8	Restriction digest.....	36
5.12	Statistical analysis .....	36
6	Results.....	37
6.1	Establishment of an AoSMC calcification assay.....	37
6.1.1	Calcification assay (high $\text{Ca}^{2+}/\text{P}_i$ ).....	37
6.1.2	Optimization of calcification assay and monitoring miR-31 expression of AoSMCs over time.....	40
6.1.3	Normalization by SYBR Green I .....	43
6.1.4	Calcification assay (low $\text{Ca}^{2+}/\text{P}_i$ ) – 1 <sup>st</sup> donor.....	44
6.1.5	Calcification assay (low $\text{Ca}^{2+}/\text{P}_i$ ) – 2 <sup>nd</sup> donor .....	51
6.2	Long-term hydrocortisone treatment .....	54
6.3	Luciferase reporter plasmid .....	55
7	Discussion .....	60
7.1	miR-31 inhibits osteoblastic transition of VSMCs in one donor.....	60
7.2	Investigating the role of hydrocortisone on the expression of miR-31 in HUVECs .....	63

8	Acknowledgements.....	64
9	References.....	64
10	Appendix .....	70
10.1	Zusammenfassung.....	70
10.2	Lebenslauf.....	71
10.3	Vector maps .....	72
10.4	List of abbreviations .....	73

## 2 Abstract

Atherosclerosis and osteoporosis are two wide-spread, age-related diseases where calcium deposition, regulated by molecular mechanisms of osteogenic differentiation, plays a key role. Recently, we found that senescent endothelial cells mitigate osteogenic differentiation of adipose-derived stem cells by secreting a microRNA, miR-31, in microvesicles. Based on this finding we tested two hypotheses. First, if miR-31 inhibits the calcification of vascular smooth muscle cells - a cell type that was shown to undergo osteogenic differentiation in arteriosclerosis, causing vascular calcification. Second, if miR-31 is up-regulated in endothelial cells upon long-term treatment with hydrocortisone (HC) - a glucocorticoid inducing osteoporosis. We observed a decrease in calcification of VSMCs transfected with miR-31 in cells from one donor. Prior to this assay we tested different concentrations of  $\text{Ca}^{2+}/\text{P}_i$  and adapted a previously published method based on staining of cells with SYBR Green I to normalize our data to DNA content. In addition, we attempted to design a luciferase reporter plasmid to identify further targets of miR-31 which remained unfinished due to time constraints. In order to investigate the long-term effect of HC on endothelial cells we incubated HUVECs with or without HC for 5 passages and determined expression of miR-31 by qPCR. Despite a significant upregulation of miR-31 in previous short-term experiments, we did not observe a significant difference in miR-31 expression between cells receiving HC and control cells.

## 3 Introduction

### 3.1 Ageing and cellular senescence

The ageing human being is challenged by several biological changes throughout its life. The individual suffers from a progressive loss of function, a decreasing fertility and increasing mortality<sup>1</sup>. There are diseases like cancer, Alzheimer's disease, type 2 diabetes, arteriosclerosis or osteoporosis to name just a few. The latter two, arteriosclerosis and osteoporosis, are two age-related diseases this thesis will address. Diseases affecting the circulatory system such as arteriosclerosis are the main causes of death for Europeans aged 65 years and older<sup>2</sup>. Even Ötzi, the iceman discovered in the Alps who lived about 5300 years ago, suffered from arteriosclerotic calcifications<sup>3</sup>. Today, the number of aged individuals is rising in many countries, accompanied by rising age-related diseases and rising health costs. To understand the regulations and underlying causes of ageing and its diseases is, therefore,

one of the major challenges biomedical research has to face in the 21<sup>st</sup> century in order to bring more health into the later years of an extended lifespan.

A first clue on how ageing might work was discovered five decades ago. Hayflick and colleagues reported that cells in culture show a limited ability to proliferate. After a period of strong cell growth proliferation stops even though cells are still provided with sufficient nutrients, growth factors and space. This condition was termed replicative senescence and is defined as a permanent cell-cycle arrest of damaged cells. Senescent cells are unable to proliferate but remain metabolically active. This in vitro behaviour of cells was soon linked to organismal ageing and there is mounting evidence that replicative senescence indeed promotes ageing<sup>4</sup>.

Besides the irreversible growth arrest, the senescent phenotype includes morphological changes<sup>5</sup> and an altered gene expression<sup>4</sup>. Potent cell-cycle inhibitors are the main cause for growth arrest and usually, but not always, leave senescent cells with a DNA content that is characteristic of G1 phase. In addition, genes responsible for cell-cycle progression are repressed. Many cell types develop a resistance to certain apoptotic signals which might explain why senescent cells accumulate with age and why they are so stable in culture. Senescence and apoptosis have one regulator in common – the tumour suppressor p53. However, the exact mechanism that leads to apoptosis resistance waits to be elucidated. Furthermore, gene expression seems to change in a way that is unrelated to growth arrest or apoptosis resistance<sup>4</sup>. Intriguingly, the secretome of senescent cells undergoes profound changes and can affect the tissue microenvironment. This phenomenon was termed the senescence-associated secretory phenotype (SASP)<sup>5</sup> - a key finding that is the basis of our work on the calcification of vascular smooth muscle cells (VSMCs). Additionally, senescent cells show expression of a senescence-associated  $\beta$ -galactosidase (SA- $\beta$ -gal)<sup>6</sup>.

Why does such a condition as cellular senescence exist? After its observation two hypotheses were established. First, cellular senescence could be a tumour-suppressive and, thus, beneficial mechanism. Second, cellular senescence in vitro may recapitulate the loss of the regenerative capacity of cells in vivo. The ability for tissue renewal deteriorates with age and cellular senescence could be the underlying cause<sup>4</sup>.

Before we discuss the various forms of cellular senescence in detail let us have a brief look at the evolutionary context of this phenomenon. Cancer can be a fatal disease and can affect an organism's longevity considerably. Uninhibited proliferation is an essential part of

tumourigenesis and cellular senescence may be a mechanism that evolved to stop cancer cells from proliferating. Due to various hazards that limited the life of a human being throughout its evolution the tumour-suppressor mechanisms had to be effective for a shorter life span compared to the longevity of modern man. The possibly disadvantageous sides of senescence, for instance reduced tissue renewal, did not come into effect and, hence, there was no selective pressure to adapt this mechanism<sup>4</sup>. Consequently, senescence can be beneficial to young organisms but detrimental to old ones. This describes the concept of antagonistic pleiotropy, an important evolutionary theory of ageing<sup>1</sup>.

Previously we have defined cellular senescence as a permanent growth arrest of damaged cells. The damage can be caused by several stressors such as shortened telomeres, non telomeric DNA damage, strong mitogenic signals, chromatin perturbations or other non-genotoxic stresses<sup>4</sup>. All these stimuli can induce different forms of cellular senescence some of which we shall discuss now in greater detail.

### **3.1.1 Replicative senescence**

After explantation of primary cells the proliferative capacity undergoes three phases. In phase I, the establishment of the culture before the first passage, the cells show little proliferation. Cells in phase II proliferate quickly whereas proliferation in phase III gradually ceases and finally comes to a complete halt<sup>7</sup>. One of the reasons for the transition from phase II to phase III is the progressive shortening of telomeres (repetitive sequences which form the protective ends of chromosomes). Since DNA polymerase is unable to replicate the lagging strand entirely, telomeres shorten each round of replication until they reach a critical minimal length. The subsequent state is termed replicative cellular senescence and the cell reached the so called "Hayflick limit"<sup>5</sup>.

Once the telomeres do not provide a protective structure for chromosomes anymore, a DNA damage response (DDR) is triggered. The interaction of the cell cycle machinery and DDR-associated factors is based on phosphorylation and activation of cell cycle proteins such as CDC25 and p53<sup>5</sup>. This process leads to a growth arrest that allows the cell to repair the DNA damage. However, if the DNA damage surpasses a certain limit the growth arrest remains permanent and the cell undergoes either apoptosis or senescence. The factors that decide which of the two possible outcomes takes place are not fully understood yet. The cell type, the nature of the damage as well as the duration and intensity of the signal seem likely to determine the outcome<sup>8</sup>.

There is, however, a way to bypass replicative senescence. Telomerase is able to add telomeric DNA repeats to shortening chromosome ends<sup>9</sup>. It consists of the catalytic protein TERT (telomerase reverse transcriptase) and an RNA template. Most cell types do not express telomerase or fail to express it at a sufficient level that maintains the length of telomeres<sup>10</sup>. On the contrary, most cancer cells and cells from the germ-line show effective TERT expression. Replicative senescence of human somatic cells can be avoided by ectopic expression of TERT. The result is an immortalized cell unable to undergo senescence caused by telomere erosion. Still there are stimuli such as non-telomeric DNA damage which can induce other forms of senescence<sup>4</sup>.

### 3.1.2 Oncogene-induced senescence

Oncogenes are mutant forms of normal genes that, together with further mutations, transform cells and, as a result, cause cancer. As a response to many oncogenes normal cells are able to undergo senescence. Oncogenes that elicit senescence usually promote cell proliferation via expression of strong mitogenic signals. Consequently, senescence may be an attempt of an incipient cancer cell to counter its transformation<sup>4</sup>.

There are similarities between oncogene-induced and replicative senescence. Both stimuli, oncogenes and eroded telomeres, induce p16<sup>4</sup> and a DDR as a result of aberrant DNA replication like misfired replication origins or replication fork collapse. The DDR, in turn, induces and maintains the senescent state<sup>11</sup>.

Oncogene-induced senescence was first described as an in vitro phenomenon in normal fibroblasts by overexpression of oncogenic H-rasV12, a cytoplasmic transducer of mitogenic signals<sup>12</sup>. Not all cells are capable of undergoing this version of senescence. Nonetheless, there is evidence that supports its role in tumour suppression in vivo. It has been shown in mice that activated oncogenes or the loss of tumour suppressors elicit benign lesions and that these lesions contain senescent cells. Similarly, senescent cells that express the oncogene BRAF were found in benign naevi in human skin<sup>4</sup>. In both cases, however, the senescent cells were prominent in the pre-malignant state but scarce when the lesions became malignant. It is yet unclear if the tumours arise out of senescent cells which reverse the growth arrest or if they arise out of nonsenescent cells that eventually bypass senescence or apoptosis<sup>11</sup>.

Interestingly, recent findings endorse the view that senescence is not only involved in tumour suppression but also in tumour promotion. This can be explained by the aforementioned SASP. Senescent cells secrete inflammatory factors which, in turn, fuel cancer progression<sup>13</sup>.



### 3.1.3 Stress induced senescence in vitro

Cells in culture have to cope with conditions that differ from those experienced in vivo. The artificial environment provides abnormal concentrations of growth factors and nutrients or lack neighbouring cell types and components of the extracellular matrix. The resulting culture shock can initiate stress-induced premature senescence (SIPS). The ambient O<sub>2</sub> level also plays a critical role. Unlike human cells, many mouse cells express telomerase and feature long telomeres (>20kb<sup>4</sup>). Nevertheless, they undergo SIPS when cultured under standard culture protocols which provide supraphysiological oxygen levels of 20%<sup>5</sup>. Human keratinocytes senesce under standard culture conditions despite long telomeres unless they are grown on feeder layers that consist of fibroblasts<sup>4</sup>.

### 3.1.4 Linking cellular senescence with ageing

Cellular senescence was first observed in vitro and has been studied mainly in cell culture in the past few decades<sup>4</sup>. Knowledge about senescent cells in vivo is now accumulating and the link between cellular senescence and ageing is currently taking shape, supported by three recent publications which we shall discuss later.

In order to identify senescent cells in vivo, markers had to be established. However, none of these markers is expressed exclusively by senescent cells. Still, the number of cells expressing one or more of senescence-associated markers is low in young organisms but increases with age. Senescent cells were found in many epithelial organs, the haematopoietic system and the vasculature and, intriguingly, at sites of chronic age-related diseases like atherosclerosis. Furthermore, there is evidence that a decline in haematopoiesis, neurogenesis and pancreatic function in mice is linked to p16-dependent senescence that leads to a suppression of stem-cell proliferation and tissue renewal. This might explain partly why brain and bone-marrow function deteriorate with age. It is, however, unclear if the p16-positive stem and progenitor cells are senescent or if the activities of p16 that fuel ageing are caused by mere growth suppression without actual senescence. Further research in mice revealed that a constitutively elevated p53 activity leads to multiple signs of premature ageing while these mice stay remarkably cancer-free<sup>4</sup>. Several other mouse models show a striking concurrence of senescent cells in vivo and age-related degenerative pathologies<sup>11</sup>.

Another important characteristic of senescent cells - the SASP - can be linked to ageing. Senescent cells secrete factors that affect cell proliferation and differentiation, tissue structure and vascularization. These factors might disrupt the structure and function of tissues. In

addition, there are many inflammatory cytokines among the secreted factors of senescent cells. This may explain the low-level chronic and 'sterile' inflammation of ageing tissues<sup>13</sup>.

A direct approach - eliminating cellular senescence and, as a result, extending life span and improving tissue function - was, until recently, not successful because organisms incapable of undergoing cellular senescence unavoidably develop cancer. Evidence linking cellular senescence with ageing was rather circumstantial<sup>11</sup>. Three recently published studies seem to have accomplished to provide this direct link.

Jaskelioff et al. took an interesting and direct approach to investigate the effect of telomerase on telomerase-deficient mice<sup>14</sup>. All mice included in the study showed significant progeroid phenotypes, for instance tissue atrophy, testicular and splenic atrophy, decreased fecundity and longevity as well as intestinal crypt depletion. The knock-in mouse model featured a 4-hydroxytamoxifen (4-OHT)-inducible TERT-oestrogen receptor and short dysfunctional telomeres. Telomerase was reactivated by applying 4-OHT for four weeks. The result was a remarkable tissue rejuvenation not seen in mice that received the vehicle. Testes and spleen were restored to a normal size. Fecundity, longevity and neural fitness increased, telomeres were elongated and DNA damage signalling stopped. It may be likely that replicative senescence contributed to the progeroid phenotype of telomerase-deficient mice, nevertheless, the study did not provide any evidence that senescent cells were found in the atrophic tissues nor did it compare the number of senescent cells in control mice with mice receiving 4-OHT.

Such evidence, however, was delivered recently by another study. Baker et al.<sup>15</sup> established a mouse model based on BubR1<sup>H/H</sup> mice which develop an age-associated phenotype characterized by infertility, sarcopenia, fat loss, cataracts, arterial wall stiffening and dermal thinning. A known marker for senescent cells - p16<sup>Ink4a</sup> - accumulates in adipose tissue, skeletal muscle and eye of these mice. A transgene was introduced to the BubR1<sup>H/H</sup> mice that enabled the efficient elimination of p16<sup>Ink4a</sup>-positive cells upon administration of the synthetic drug AP20187. These cells also proved to express other senescence-associated markers. Early-life treatment led to a delayed onset of sarcopenia and cataracts, larger muscle fibre diameters and an increased performance in treadmill exercise tests compared with untreated mice. Moreover, the loss of adipose tissue was prevented. The treatment did not have an effect on longevity which the authors argue is due to the fact that most BubR1<sup>H/H</sup> mice die of cardiac failure. Heart and aorta consist of tissues that do not express p16<sup>Ink4a</sup> when undergoing senescence. Inguinal adipose tissue, skeletal muscle and eye of AP20187-treated mice showed

a decrease in senescence-related markers. The clearance of p16<sup>Ink4a</sup>-positive cells later in life did not reverse the age-related decline but attenuated its progression.

One could argue that these two in vivo studies are based on mouse models that develop progeroid phenotypes early in life and that the knock-in of telomerase or the clearance of p16<sup>Ink4a</sup>-positive cells just reverses this artificial phenotype. Another study published last month by Bernardes de Jesus et al.<sup>16</sup>, however, demonstrates similar beneficial effects of a telomerase gene therapy on normal C57BL/6 mice. An adeno associated virus of wide tropism introduced telomerase in 1- and 2-year old mice. The result was a remarkable increase in median lifespan, health and fitness. The improvement was also detectable on molecular biomarkers of ageing. Moreover, telomerase-treated mice did not show an increased cancer rate compared to their control littermates. Introduction of a catalytically inactive form of mTERT did not have any effect, suggesting that elongation of telomeres led to the improved health.

In conclusion, the link between ageing and cellular senescence is currently taking shape. Despite mounting evidence that senescent cells drive ageing, there are also other factors that certainly contribute to age-related diseases - apoptosis, for instance, or the simple loss of functionality of cells<sup>11</sup>.

### 3.2 The ageing blood vessel

There are many risk factors in life for developing cardiovascular diseases (CVDs) like stroke, congestive heart failure, hypertension or atherosclerosis. Among them one can find genetic factors, diabetes, dyslipidemia or a sedentary lifestyle. Advanced age, however, is the main risk factor<sup>17</sup>. As mentioned above, CVDs are the main cause of death in aged individuals. Before we take a close look to the various changes the vasculature experiences with advancing age let us familiarize ourselves briefly with the blood vessel.

The artery consists of three layers called the tunica intima, tunica media and tunica adventitia (Figure 1). The inner coat - the one that has direct contact with the blood stream - is called the tunica intima, or intima. It consists of a single layer of plain endothelial cells which is supported by an elastic, fenestrated membrane (internal elastic lamina). The middle layer, termed the tunica media or media, mainly consists of VSMCs and elastic fibres. Tunica adventitia, also known as tunica externa, is the outermost layer and consists of connective tissue. It anchors the blood vessel to the surrounding tissue and in some cases is supported by a thin elastic membrane called the external elastic lamina<sup>18</sup>.

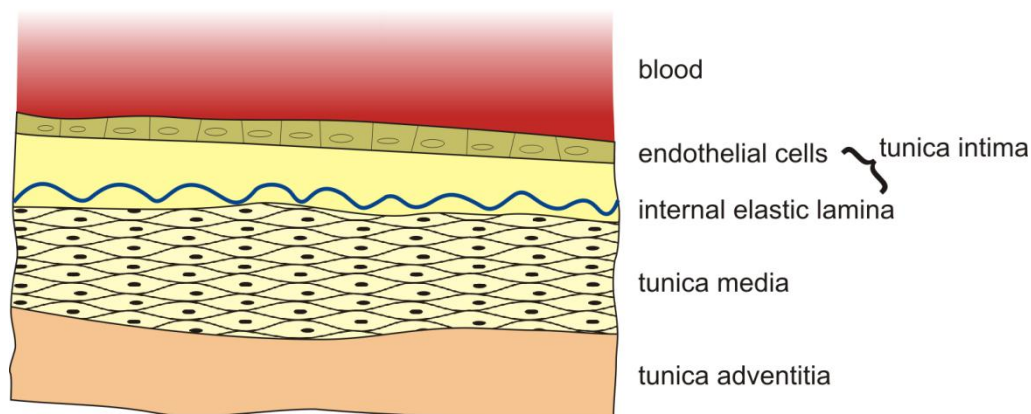


**Figure 1.** Anatomy of a large artery. The arterial wall consists of three layers called intima, media and adventitia. The normal intima usually is thinner; its size is exaggerated in this figure. Vascular smooth muscle cells are located in the media.

The blood vessel undergoes several age-related alterations. It is, nonetheless, difficult to distinguish between changes caused by age per se and changes caused by cardiovascular or noncardiovascular diseases such as diabetes, borderline hypertension, thyroid dysfunction or heart failure. Surprisingly, age-related changes in the cardiovascular system do not always prove to be a decline in function. Some of them not only remain unimpaired but rather become enhanced in age<sup>19</sup>.

First, let us have a look at the structural changes of the vasculature. Large arteries like the aorta have an enlarged lumen and become stiffer, elongated and tortuous<sup>19</sup>. The arterial wall thickens which primarily affects the intima and the media, with the thickening in the intima being more pronounced<sup>20</sup>. Endothelial cells can show an irregular shape and an increased height. Healthy elderly subjects do not show endothelial lesions or discontinuities. VSMCs may infiltrate the subendothelial space where

an excessive deposition of proteoglycans and collagen can be observed. In addition, an unusually high number of macrophages and other leukocytes can be found. The ageing arterial intima may also secrete several substances involved in atherosclerosis and

age-related vascular changes <sup>19</sup>	
Arterial wall thickness (intima-media)	↑
Subendothelial collagen	↑
Elastin	↓
Elastin fragmentation	↑
Proteoglycans	↑
Matrix metalloproteinase activity	↑
Intimal migration/proliferation of VSMCs	↑
Arterial distensibility	↓
Pulse wave velocity	↑
Total peripheral resistance	↑
Endothelial permeability	↑
Endothelial nitric oxide release	↓
Inflammatory markers/mediators	↑
Superoxide dismutase activity	↓
Adrenergic-mediated vasodilation	↓

**Table 1.** ↑ increase, ↓ decrease

inflammation, for instance proinflammatory cytokines, transforming growth factor- $\beta$  (TGF- $\beta$ ), matrix metalloproteinases, adhesion molecules<sup>19</sup> and IL-8<sup>21</sup>.

Along with structural changes come functional changes. The deteriorating elasticity of arteries results in the impairment of the cushioning function of the aorta and its major branches. As mentioned before, aged arteries show increased stiffness which is partly dependent on endothelial and humoral regulation of vascular smooth muscle tone<sup>19</sup>. The endothelium sees a decline in its function as a barrier and, thus, plasma proteins are able to cross into the media which contributes to the arterial thickness<sup>22</sup>. The endothelial dysfunction is in part due to the increased production of reactive oxygen species (ROS)<sup>23</sup>. A summary of the structural and functional changes of the vasculature can be found in Table 1<sup>19</sup>.

All these changes can be found in aged individuals that do not show any signs of CVDs such as atherosclerosis. Nevertheless, they form the basis on which CVDs can prosper<sup>17</sup>. Most of these age-related characteristics can also be found in atherosclerotic blood vessels which, in addition, develop focal lesions, vessel stenosis (narrowing) and plaque rupture<sup>19</sup>. A contribution to a better understanding of the processes of arteriosclerosis was one of the major goals of this thesis. The term arteriosclerosis frequently leads to misunderstandings because it is often used interchangeably with the term atherosclerosis. However, these two terms are different. Arteriosclerosis sums up three different lesions: atherosclerosis, Mönckeberg medial calcific sclerosis and arteriolosclerosis<sup>24</sup>.

*Atherosclerosis* is defined as a lesion of large and elastic muscular arteries that develop an atheroma. The atheroma is a swelling of the arterial intima that consists of macrophages, lipids (e.g. cholesterol), connective tissue and calcium deposits. *Mönckeberg medial calcific sclerosis*, also known as Mönckeberg's sclerosis, is characterized by a calcification of the tunica media of large and medium-sized arteries. It rarely occurs in patients younger than 50 years. Whether Mönckeberg's sclerosis involves the calcification of the internal elastic lamina - considered a part of the intima - or not is currently discussed in the field. *Arteriolosclerosis*, unsurprisingly, affects arterioles and is associated with diabetes mellitus, chronic kidney disease and hypertension<sup>24</sup>.

Calcification of VSMCs occurs in both atherosclerosis and Mönckeberg's sclerosis. Atherosclerosis, in short, starts with the aggregation of low density lipoprotein (LDL) in the intima where it is prone to oxidation. Monocytes transmigrate across the endothelium into the intima, differentiate into macrophages, absorb the oxidised lipoprotein and become so called

foam cells. The resulting 'fatty streaks' in the artery have a fibrous cap consisting of extracellular matrix produced by VSMCs that migrated from the media into the intima where they start to proliferate and calcify. The fibrous cap surrounds a lipid-rich 'necrotic core'. Ultimately, the plaque can cause a narrowing of the vessel (stenosis) or ruptures, leading to thrombosis and infarction or stroke<sup>25</sup>.

Mönckeberg's sclerosis is highly associated with cardiovascular mortality. It contributes to arterial stiffness which elicits increased pulse pressure and left ventricular atrophy<sup>26</sup>. Atherosclerosis is the leading cause of deaths in western countries. It is, therefore, important to understand the process that leads to the calcification of VSMCs. We shall discuss vascular calcification and its controversial role in atherosclerosis in detail in another chapter where we elucidate its similarity to bone formation. Prior to this, let us have a look how cellular senescence may contribute to vascular ageing.

### 3.3 Cellular senescence in cardiovascular diseases

At first glance, replicative senescence of endothelial cells seems unlikely to play an important role in CVDs because cell proliferation in the endothelium is very low. However, in parts of the vasculature susceptible to atherosclerosis - bifurcations and branching points - cell turnover is increased. At these sites, the bloodstream causes forces of shear and stretch which may be a source of chronic injury. The endothelium may respond with a higher cell turnover to maintain its integrity. Hence, senescent endothelial cells could accumulate especially at these sites. Besides telomere erosion, ROS produced by activated phagocytes or vascular cells themselves are another source of stress that may contribute to cellular senescence<sup>27</sup>.

Indeed, senescent endothelial cells confirmed by SA- $\beta$ -gal staining have been found in vivo on the surface of atherosclerotic lesions<sup>28,29</sup>. Another study demonstrates that coronary endothelial cells taken from atherosclerotic lesions have shorter telomeres compared with cells of healthy surrounding tissue<sup>30</sup>. Homocysteine, a risk factor for atherosclerosis, enhances telomere shortening and accelerates cellular senescence of endothelial cells in vitro<sup>31</sup>. Once senescent, endothelial cells show an increased interaction with monocytes. This is probably due to the upregulation of adhesion molecules and may promote atherogenesis. Another source for the aforementioned ROS is mitochondrial dysfunction. Young patients with a mitochondrial disease often suffer from vascular complications without being exposed to further risk factors for atherosclerosis. A correlation between mitochondrial DNA damage and the extent of atherosclerosis was observed<sup>32</sup>.

Not only senescent endothelial cells but also senescent VSMCs can be found in advanced atherosclerotic plaques. They are, however, confined to the intima, possibly a result of enhanced replication in the plaque<sup>32</sup>. VSMCs taken from atherosclerotic fibrous caps express markers of cell senescence and show a senescent morphology. They exhibit oxidative DNA damage and shorter telomeres compared with VSMCs taken from tunica media. This suggests that not only increased proliferation but also oxidative stress-induced DNA damage is a source of cell senescence. Furthermore, the rate of telomere attrition is positively correlated with the severity of atherosclerosis<sup>33</sup>. Burton et al. investigated the senescent phenotype of VSMCs by microarray analysis and observed that various genes up-regulated in atherosclerotic plaques are also highly up-regulated in senescent VSMCs<sup>34</sup>. Many genes that are involved in the development of atherosclerosis are differentially regulated upon senescence. Among them they discovered genes important in inflammation, tissue remodelling and vascular calcification. Another study similarly revealed that VSMCs in culture undergo a senescence-mediated osteoblastic transition and, hence, enhance calcification<sup>35</sup>.

Recent work of our group investigated the SASP of endothelial cells (data not published yet). Upon senescence, HUVECs (human umbilical vein endothelial cells) enhance expression of miRNA-31 secreted in microvesicles. When applied to ASCs (adipose-derived stem cells) microvesicles from senescent HUVECs significantly reduce osteogenic differentiation of ASCs compared to the application of microvesicles from early-passage HUVECs. This suggests that endothelial cell senescence contributes to age-related osteoporosis. Questioning why endothelial cells up-regulate a miRNA inhibiting osteogenic differentiation, we hypothesized that senescent endothelial cells attempt to reduce calcification of neighbouring VSMCs (Figure 2). Calcification of VSMCs shows remarkable similarities to bone calcification.

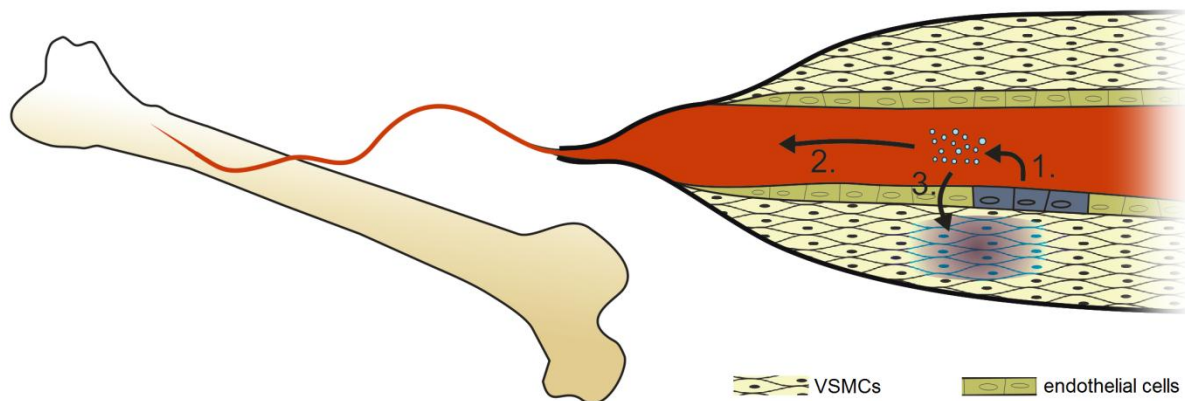


**Figure 2.** The working hypothesis this thesis is based on: (1) senescent endothelial cells (grey) secrete miR-31-enriched microvesicles that (2) reach mesenchymal stem cells in the bone via the blood stream where they inhibit their osteogenic differentiation. Microvesicles also target neighbouring VSMCs (3) where they attempt to reduce the calcification (brown) of the tunica media via miR-31.

As mentioned before, calcification of VSMCs occurs in age-related diseases such as atherosclerosis and Mönckeberg's sclerosis. Our findings suggest a role of miR-31 in the calcification of bone and - due to the similarity to calcification of VSMCs - vasculature. It is, therefore, important to understand the process of vascular calcification and how miRNAs like miR-31 may play a role in ageing and CVDs.

### 3.4 Calcification in vasculature and bone

#### 3.4.1 Clinical relevance of atherosclerotic calcification

The clinical relevance of atherosclerotic calcification and its contribution to plaque rupture is still a matter of debate. Plaque rupture is considered to be responsible for most myocardial infarctions and stroke. In general, the more calcification is observed in coronary arteries, the more significant becomes coronary stenosis. Vascular calcification as detected in patients by radiography is an accepted and sensitive marker for atherosclerosis<sup>36</sup>.

How does the calcification affect plaque stability? Abedin et al. hypothesize that the impact of calcification on plaque stability can be divided into two phases based on mechanical considerations. The mechanical stress acting on the plaque is highest at interfaces between tissues of different stiffness, in this case calcified plaque and cellular plaque. In the first phase, calcified spots occur on the plaque and create areas of interface leading to high risk of rupture. With increasing calcification, calcified spots coalesce and interface area decreases. This marks the second phase where the risk of rupture is declining<sup>36</sup>. On the contrary, another study suggests that plaques are less prone to rupture when calcified. Nonruptured plaques



exhibited more deep calcification than ruptured ones, but no difference in superficial calcium deposits was found<sup>37</sup>. The position of the calcification with regard to the plaque and the necrotic core seems to be an important factor of plaque stability<sup>38</sup>.

### 3.4.2 Bone calcification

Our understanding of how the calcification of the vasculature works has experienced a crucial change in the past decade. It was believed to be a process of passive precipitation of mineral crystals. Instead, recent findings describe it as an actively regulated process that is, as mentioned above, similar to bone mineralization. Osteoblasts are the cells mainly responsible for the formation of bones. They produce the extracellular proteins type I collagen, alkaline phosphatase and osteocalcin, the expression of the latter often considered characteristic for osteoblasts. The extracellular matrix is mainly composed of type I collagen and is called osteoid if not yet mineralized. Mineralization happens via the accumulation of hydroxyapatite that contains calcium and inorganic phosphate<sup>39</sup>.

The differentiation of mesenchymal stem cells into osteoblasts is a highly regulated process with Runx2 (Runt-related transcription factor 2, also known as Cbfa1) considered the key transcriptional factor<sup>40</sup>. Runx2<sup>-/-</sup> mice lack any signs of ossification<sup>41,42</sup>. Further differentiation of osteoblasts into osteocytes, however, is inhibited by Runx2, causing osteopenia and multiple fractures when overexpressed in mice. Overexpression led to an increase in immature osteoblasts but caused a decrease in mature osteoblasts and osteocytes<sup>43</sup>. Expression of Runx2 seems to be essential for another important transcription factor in bone formation named osterix. Differentiation into osteoblasts and bone formation is impaired in osterix null mice while Runx2 is still expressed at a normal level. In contrast, there is no expression of osterix in the absence of Runx2<sup>44</sup>. Osterix is critical not only during embryonic development but also for postnatal differentiation and function of osteoblasts and osteocytes<sup>45</sup>. Furthermore, the tumour suppressor p53 was found to repress osterix expression<sup>46</sup>.

Several developmental signals regulate the aforementioned transcription factors - hedgehog, notch, FGF, BMP and Wnt signalling. Wnt signalling can be either dependent on or independent of  $\beta$ -catenin. In the case of  $\beta$ -catenin-dependent Wnt signalling, Wnt binds to a membrane-bound receptor of the frizzled family (Fzd) which stabilizes cytosolic  $\beta$ -catenin.  $\beta$ -catenin translocates to the nucleus where it initiates the transcription of Wnt target genes. The differentiation towards mature osteoblasts requires  $\beta$ -catenin. BMPs (bone morphogenetic proteins) also play a critical role in the differentiation of osteoblasts with BMP2 being

important for postnatal bone formation<sup>39</sup>. Osterix is regulated by BMP2 via Runx2 and Msx2<sup>47</sup>.

Further regulatory factors involved in bone calcification have been determined, among them alkaline phosphatase (ALP), matrix Gla protein (MGP) and inorganic pyrophosphate (PP<sub>i</sub>). MGP and PP<sub>i</sub> both inhibit the mineralization of the extracellular matrix. ALP is able to cleave PP<sub>i</sub> and, thus, promotes bone calcification. The above described regulatory factors have also been found in blood vessels, in particular at sites of medial sclerosis. A differentially regulated expression can be observed when comparing diseased arteries with non-diseased<sup>40</sup>.

### 3.4.3 Osteoblastic transition of VSMCs

VSMCs seem to be the key players in calcification as seen in atherosclerosis and Mönckeberg's sclerosis. Mice deficient for MGP exhibit strong medial calcification and die of haemorrhaging and vascular rupture<sup>48</sup>. MGP is a circulating protein and is expressed by VSMCs. Rescuing MGP expression exclusively in VSMCs of MGP<sup>-/-</sup> mice via the SM22 $\alpha$  promoter avoids medial calcification which further shows that production of MGP locally by VSMCs is sufficient to prevent mineralization of the tunica media<sup>49</sup>. Membrane-bound matrix vesicles released by VSMCs have been linked to calcification in vivo and they were shown to contain MGP and fetuin-A, another potent and circulating inhibitor of calcification, in an in vitro study<sup>50</sup>. The same study demonstrated that apoptotic bodies also play a role in calcification and that inorganic phosphate induces VSMC calcification<sup>50</sup>. Uremic serum, as seen in patients with chronic kidney disease who frequently suffer from vascular calcification, was shown to contain higher levels of BMP2, inducing calcification of VSMCs in vitro via induction of Runx2<sup>51</sup>. Dedifferentiated VSMCs - the state in which they migrate into the intima during formation of atherosclerotic lesions - were demonstrated to up-regulate expression and secretion of BMP2 and, thus, inducing other osteogenic signals that contribute to the atherosclerotic intimal calcification<sup>52</sup>. These dedifferentiated VSMCs, however, did not exhibit an osteoblast-like phenotype as seen with differentiated VSMCs<sup>52</sup>.

Another inducer of Runx2 expression and VSMC calcification is H<sub>2</sub>O<sub>2</sub><sup>53</sup>. However, it is possible that DNA damage caused by oxidative stress triggered SIPS which, in turn, mediated the osteoblastic transition. As mentioned earlier, senescent VSMCs have been shown to undergo an osteoblastic transition, expressing many bone calcification

regulatory factors. Nakano-Kurimoto et al. investigated the phenotype of senescent VSMCs extensively in vitro<sup>35</sup>. Senescent VSMCs exhibit upregulation of Runx2, ALP and type I collagen compared to early-passage VSMCs. Runx2 fulfils its function as a key transcription factor also in senescent VSMCs. Its knockdown resulted in weaker VSMC calcification with lower levels of ALP. Knockdown of either type I collagen or ALP also reduced VSMC calcification. Surprisingly, the expression of osterix is decreased despite elevated levels of Runx2. Osteocalcin, a marker for mature osteoblasts, is not elevated in senescent VSMCs. The authors explain this with the expression of osteocalcin being reported as synchronous with osterix<sup>54</sup> and that senescent VSMCs represent osteoblast-like cells rather than fully differentiated osteoblasts. MGP, the potent inhibitor of calcification, is significantly down-regulated in the senescent state<sup>35</sup>. A study published by Burton et al.<sup>34</sup> at the same time confirms these observations about the senescent phenotype of VSMCs except for BMP2 which Burton et al. reported as elevated 3-fold rather than unaltered. Investigation of Runx2 expression in vivo in arteries with medial calcification revealed an increase particularly where calcification was detected<sup>35</sup>. A part of the senescent phenotype of VSMCs is summarized on Table 2.

the senescent phenotype of VSMCs <sup>34,35</sup>	
alkaline phosphatase (ALP)	↑
BMP2	?
matrix gla protein (MGP)	↓
osteocalcin	-
osteopontin	↑
osterix	↓
Runx2	↑
type I collagen	↑

**Table 2.** ↑ upregulation, ↓ downregulation, ? conflicting results, - unaltered

Besides these factors, there are further regulators of osteogenic differentiation. As discussed above, our group found a microRNA being up-regulated during senescence of endothelial cells and inhibiting osteogenic differentiation. Not only miR-31 but also other miRNAs have been determined to be involved in bone formation. Moreover, miRNAs have been found to play an important role also in ageing and age-related diseases.

### 3.5 MicroRNAs

MicroRNAs are non-coding RNAs consisting of approximately 21 nucleotides. They are able to regulate the translation of mRNAs as well as their localization and polyadenylation. miRNAs bind to complementary sequences within their target mRNA and negatively

modulate the gene expression post-transcriptionally. They play a critical role in many biological events such as proliferation, differentiation, apoptosis, tumourigenesis and, not to forget, ageing and bone remodelling<sup>55,56</sup>.

Genes encoding miRNAs can be found on every human chromosome except for the Y chromosome. miRNA genes can be independent genes or can be localized in introns of other protein-coding or non-protein-coding genes. Transcription of miRNA genes is done by either RNA Pol II or Pol III, its regulation works through transcription factors or epigenetics. The transcript is called primary miRNA (pri-miRNA), can be several 1000 nucleotides in length and may contain multiple miRNAs that are being co-transcribed (Figure 3<sup>57</sup>). Just as mRNAs, the pri-miRNA is capped and polyadenylated. Still in the nucleus, a complex consisting of Drosha and DGCR8 (DiGeorge syndrome critical region gene 8) processes the pri-miRNA. The pri-miRNA forms an imperfect stem-loop that enables recruiting and binding by DGCR8. Drosha, an RNase III-type endonuclease, then cleaves the pri-miRNA, leaving a stem-loop precursor miRNA (pre-miRNA) of approximately 60 to 100 nucleotide length. Exportin5 ensures the transport of the pre-miRNA from the nucleus to the cytoplasm. Exceptions to this pathway are mirtrons. Mirtrons are miRNAs located between two exons of another gene. Debranched and spliced, they bypass cleavage by Drosha and enter the canonical pathway of miRNA biogenesis after nuclear exportation<sup>56</sup>.

Once in the cytoplasm, a complex of Dicer and TRBP (TAR RNA binding protein) further processes the pre-miRNA. Similar to Drosha/DGCR8, TRBP recruits and binds the pre-miRNA, whereas Dicer is an RNase III-type endonuclease cleaving the pre-miRNA. Cleavage by Dicer requires the pre-miRNA stem-loop to contain central mismatches. The result is an approximately 21 nucleotide long miRNA duplex that becomes incorporated into another complex called RISC (RNA-induced silencing complex) that, among other proteins, includes Dicer. Helicases unwind the duplex into two single strands. One strand becomes the guide strand (pink in Figure 3), the other one is the passenger strand miRNA\* which most often is degraded by the RISC. Some miRNAs\*, however, remain functional and also regulate gene expression<sup>56</sup>.

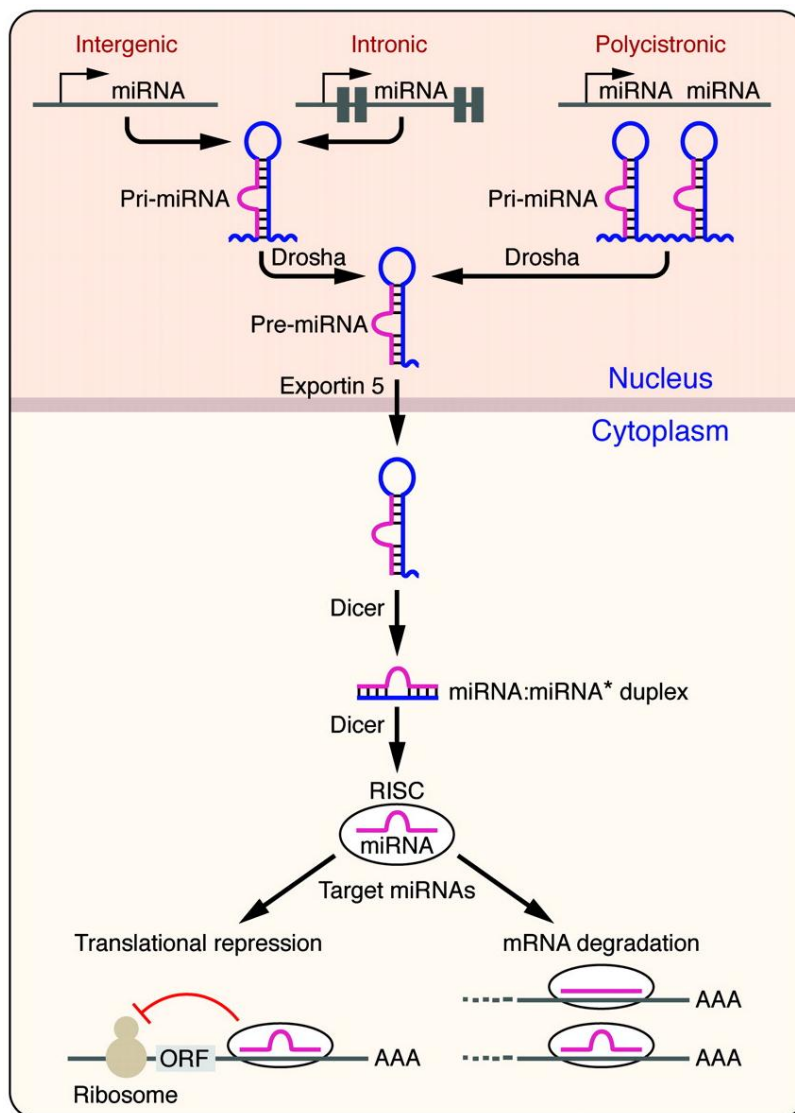


**Figure 3.** The pathway of miRNA biogenesis. Picture copied with kind permission of Eva van Rooij<sup>54</sup>. miRNA genes can be located either intergenic, intronic or poly-cistronic. Transcription of the gene results in a pri-miRNA which is cleaved by Drosha (+DGCR8), producing a pre-miRNA of approximately 60 to 100 nucleotide length. After exportation into the cytoplasm by Exportin 5, Dicer (+TRBP) cleaves the imperfect stem-loop, producing a duplex of about 21 nucleotides length. RISC delivers the guide strand (pink) to the target of the miRNA. The target can either be degraded or its translation can be repressed.

The RISC then delivers the guide strand to the target mRNA. Base pairing mainly occurs at the 3'UTR (untranslated region) of the mRNA. A few exceptions have been found that bind to the 5'UTR or within the translated region of the mRNA. Binding is crucial in the so called seed region of the miRNA (nucleotides 2 to 8). Perfect binding leads to the degradation of the target mRNA. Most miRNAs, however, bind imperfectly to their target with a bulge between nucleotide 9 and 11. This results in translational repression by blocking the interaction of eIFs (eukaryotic initiation factors) or binding to the 5'cap of the mRNA. RISC-miRNA can also bind to mRNAs that are already actively translated which reduces elongation or leads to enhanced termination<sup>56</sup>.

### 3.5.1 MicroRNAs in ageing and cardiovascular diseases

The first miRNA ever discovered, lin-4 in *Caenorhabditis elegans*, was also the first being linked to the regulation of ageing a few years ago. Since then many other miRNAs have been

found to be significantly up- or down-regulated in ageing. Many of these miRNAs play a role as regulators of ageing on the level of the organism, tissue or cellular senescence. A lot of work has been done in *C. elegans* revealing miRNAs associated with the nematode's lifespan. Nevertheless, miRNAs involved in mammalian ageing also have been found. A plethora of miRNAs are differentially expressed when comparing old versus young tissues. Research in mice has revealed various miRNAs being up-regulated in aged liver (e.g. miR-34a, miR-93, miR-214), brain (e.g. miR-22, miR-101a, miR-720) and skeletal muscle (e.g. miR-7, miR-468, miR-542). There are miRNAs targeting both factors promoting longevity and factors antagonizing longevity. Moreover, miRNAs have been linked to cellular senescence as regulators by targeting factors involved in the response to senescence-inducing cellular stress (e.g. oxidative stress) or in tumour-suppressor pathways<sup>58</sup>.

miRNAs are also important in signalling and function of vascular cells like endothelial cells or VSMCs. Many of these miRNAs are deregulated in CVDs such as atherosclerosis or coronary artery disease. Several miRNAs play a role in the differentiation of VSMCs. miR-24, for instance, functions as a mediator of the contractile phenotype of VSMCs. As mentioned before, VSMCs can switch between a differentiated (contractile) state and a dedifferentiated (proliferative, synthetic) state in which they are able to migrate into the intima as seen in atherosclerosis. A critical regulator of this phenotype shifting of VSMCs is miR-26a which promotes proliferation and migration while inhibiting differentiation and apoptosis<sup>59</sup>. Another activator of VSMC proliferation is miR-146a which also promotes neointimal hyperplasia. On the contrary, the miR-143/145 cluster represses proliferation and promotes differentiation of VSMCs and is down-regulated in some CVDs, among them atherosclerosis. Taken together, miRNAs seem to play an important role in modulating the VSMC phenotype which suggests the development of therapies against proliferative CVDs based on miRNAs<sup>59</sup>.

### **3.5.2 miRNA-31**

According to Valastyan et al.<sup>60</sup> there are more than 200 mRNAs predicted in silico to be a target of miR-31. Many of these targets are genes involved in processes linked to motility like cytoskeletal remodelling, cell adhesion and cell polarity. Research done on miR-31 so far established its relevance mainly in cancer. For instance, miR-31 acts as an inhibitor of breast cancer metastasis<sup>60</sup>. Furthermore, it is down-regulated in highly malignant prostate cancer cell lines compared to benign prostate cancers. It targets antiapoptotic E2F6 promoting apoptosis induced by chemotherapeutic agents. The downregulation of miR-31, thus, may be involved

in apoptosis resistance of prostate cancer cells<sup>61</sup>. In lung cancer, miR-31 increases proliferation and tumorigenicity of lung cancer cells and was confirmed to target Dickkopf-1 (Dkk-1) and DACT-3<sup>62</sup>. Moreover, miR-31 expression is enhanced in oral carcinoma, measurable in the saliva of cancer patients and, hence, serving as a potential biomarker of oral squamous cell carcinoma<sup>63</sup>. It is differentially regulated in other cancers such as glioblastoma<sup>64</sup> or pancreatic cancer<sup>65</sup>.

Apart from cancer, miR-31 was linked to various other processes. FOXP3 (forkhead box P3), involved in the regulation of regulatory T cells, is a direct target of miR-31<sup>66</sup>. Intriguingly, BMP2 was shown to induce upregulation of miR-31 in mouse embryonic mesenchymal cells<sup>67</sup>. Controlling of gene expression in murine skin and hair follicle was also associated with miR-31, revealing several factors of the BMP and Wnt pathway as its target<sup>68</sup>. Other studies link miR-31 with the regulation of neutrophil adhesion<sup>69</sup>, adipogenic differentiation in rats<sup>70</sup> and, interestingly, osteogenic differentiation<sup>71</sup>. Zhang et al. recently published that miR-31 is down-regulated during osteogenic differentiation of human ASCs<sup>71</sup> which is consistent with our finding of miR-31 inhibiting osteogenic differentiation of ASCs which makes it a likely player in the development of osteoporosis.

### **3.6 Cortisol-induced osteoporosis**

Glucocorticoids (GCs) are used to treat a variety of diseases, e.g. rheumatoid arthritis or polymyalgia rheumatica. They elicit, however, severe side effects such as hypertension, insulin resistance, glaucoma and osteoporosis. One of these GCs frequently prescribed is hydrocortisone (cortisol, HC). A meta-study revealed that about 3% of the population older than 50 years has taken GCs which leave the patients with a higher risk of fractures and bone loss. 30% of patients taking a GC more than 6 months develop osteoporosis. The GC-induced bone loss is divided in two phases - a rapid first phase with bone loss of 3 to 5% in the first year of treatment and a slower second phase with 0.5 to 1% annual bone loss during continued use. Moreover, 30% of patients on chronic GC treatment suffer from an incident fracture. GCs act on several pathways by binding to a cytosolic GC receptor. This leads to the translocation into the nucleus where they regulate various transcription factors<sup>72</sup>. The mRNA levels of type I collagen and osteocalcin are reduced by GCs and it has been shown that they modulate the expression of osteopontin, bone sialoprotein, fibronectin and insulin-like growth factors<sup>73</sup>. Ultimately, GCs lead to an enhanced apoptosis of osteoblasts and osteocytes via activation of caspase-3, a decreased differentiation of osteoblasts and a higher life span of osteoclasts (responsible for bone resorption). All this results in a critical decline of bone formation.

Instead of osteogenic differentiation, GCs promote a shift towards the adipogenic pathway. Furthermore, it was shown that GCs inhibit Runx2 and suppress the Wnt signalling pathway by increasing the expression of Dkk-1. Silencing Dkk-1 inhibits the ability of GCs to suppress the differentiation of osteoblasts<sup>72</sup>.

As mentioned earlier, miR-31 was found to inhibit osteogenic differentiation of ASCs in vitro (data not published yet). Senescent endothelial cells up-regulate secretion of miR-31 in microvesicles, suggesting a role of miR-31 in age-related osteoporosis. Treatment with hydrocortisone exposes endothelial cells to this inducer of osteoporosis. Hence, we hypothesized that hydrocortisone leads to an upregulation of miR-31 in endothelial cells, contributing to the development of osteoporosis. Indeed, in a short-term experiment, HC led to an upregulation of miR-31 within 24 hours (not published yet).



## 4 Aims

The aim of this thesis was to establish a role for miR-31 in two widespread diseases - arteriosclerosis and cortisol-induced osteoporosis. Unpublished work of our group showed that miR-31 is up-regulated in senescent endothelial cells and secreted in microvesicles. These microvesicles inhibit the osteogenic differentiation of ASCs which suggests that miR-31 is involved in age-related osteoporosis. Osteoporosis is a known and severe side effect of long-term HC treatment. We hypothesized that HC leads to an upregulation of miR-31 in endothelial cells and that miR-31, hence, contributes to the development of cortisol-induced osteoporosis. Previously, we observed an upregulation of miR-31 in HUVECs upon short-term treatment with HC. Therefore, we investigated the long-term effect of HC on the expression of miR-31 by HUVECs in vitro.

Our data also suggest that miR-31 may be involved in arteriosclerosis. In both atherosclerosis and Mönckeberg's sclerosis VSMCs undergo osteogenic differentiation which leads to the calcification of the arterial intima or media respectively. We hypothesized that miR-31-enriched microvesicles of senescent endothelial cells target neighbouring VSMCs to inhibit their osteogenic differentiation and, thus, mitigate their ability to calcify. Hence, we investigated whether transfection of aortic smooth muscle cells (AoSMCs) with miR-31 leads to a weaker calcification. Ultimately, a confirmed negative effect of miR-31 on osteogenic differentiation of VSMCs could be of clinical use in the treatment of the aforementioned diseases.

Fzd3, a co-receptor involved in WNT signalling, is a confirmed target of miR-31<sup>60</sup>. To determine whether further regulatory factors in osteogenic differentiation are targets of miR-31 we attempted to design a luciferase reporter construct in which the 3'UTR of putative targets of miR-31 can be cloned. In case of positive targeting transfection of miR-31 would lead to a lower secretion of luciferase into the culture medium which can be detected easily.

## 5 Materials and methods

### 5.1 Measurement of calcium-content and SYBR Green I staining

The calcification of AoSMCs was measured as described previously<sup>74,75</sup>. The accumulated calcium was dissolved by incubation of cells in 0.6 M HCl. The amount of calcium in the supernatant was quantified with a kit based on the o-cresolphthalein complexone method. Together with calcium, ortho-cresolphthalein complexone builds a complex of purple colour, which can be detected photometrically. For normalization to DNA-content a previously described method was applied with minor modifications<sup>76</sup>. After incubation with 0.6 M HCl, the cells remain in the well and are incubated with SYBR Green I, a dye that preferentially binds to double-stranded DNA. The quantification of calcium was normalized to the FI results (fluorescence intensity) of the SYBR Green I staining (Figure 4).

For the standard curve of SYBR Green I staining the following numbers of AoSMCs were seeded in two 12-well-plates in duplicates:  $5.5 \times 10^4$ ,  $6.0 \times 10^4$ ,  $6.5 \times 10^4$ ,  $7.0 \times 10^4$ ,  $7.5 \times 10^4$ ,  $8.0 \times 10^4$ ,  $8.5 \times 10^4$ . Cell count was taken before seeding in the cells using a Bürker-Türk counting chamber. The individual duplicates were seeded on two different plates to see if the FI-values on different plates are comparable. As soon as the AoSMCs were attached to the well, cells were treated according to the following protocol:

- remove media
- wash 3 times with PBS w/o Ca & Mg (1 ml/well)
- add 0.6 M HCl (0.5 ml/well), incubate o/n at 4°C
- take HCl and measure the Calcium-content with Quantichrom Calcium Assay kit according to the manufacturer's protocol
- wash 1x cautiously with PBS (1 ml/well)
- add 70 % EtOH (ice-cold, 1 ml/well), incubate for 2.5 h at -20°C
- remove EtOH
- wash 1x with PBS (1 ml/well)
- for permeabilization add 0.5 ml/well of the following solution:
  - 0,1 % Triton X-100
  - 50 mM Tris-HCl pH 7.4
  - 150 mM NaCl
  - 5 mM EDTA
  - 0.1 % gelatine

- 0.05 % Nonidet P40
- diluted in dH<sub>2</sub>O
- incubate 30 min at RT
- remove permeabilization-solution and wash 1x with PBS (1 ml/well)
- add SYBR Green I solution (1:10.000 in PBS, 0.5 ml/well)
- wrap plate in aluminium foil and incubate at RT for 4 h or o/n at 4°C
- measure Fluorescence Intensity with TECAN-Reader (without lid):
  - Multiple Reads per Well (filled circle): 5x5
  - border: 4 mm
  - Excitation Wavelength: 488 nm
  - Emission Wavelength: 522 nm

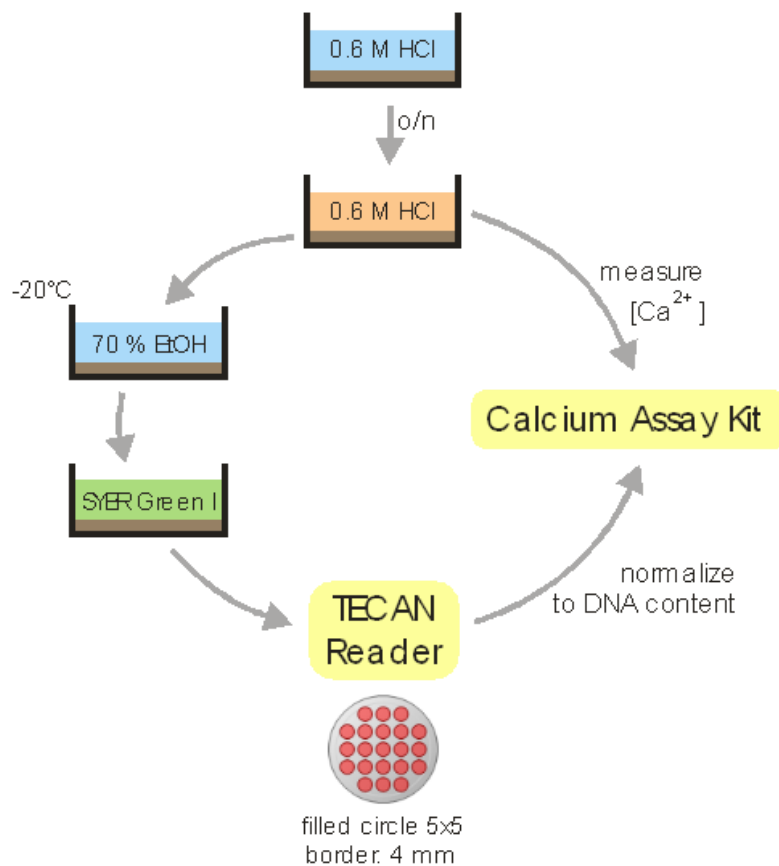


**Figure 4.** Procedure of how the calcification of AoSMCs is measured and normalized to the DNA-content.

## 5.2 RNA-Isolation

### Harvest cells

- harvest cells (protocol depends on cell type)
- transfer cell suspension to a new RNase free Sarstedt tube
- spin cells down (10 min, 170 g)
- discard supernatant (keep the pellet)

### Homogenisation

- add 500 µl TRIzol reagent (Invitrogen) to harvest cells
- homogenize by pipetting up and down
- incubate at room temperature for 5 min.

### Phase separation

- cool down centrifuge to 4°C
- add 200 µl chloroform to each tube
- vortex for 15 seconds
- incubate for 2-3 min. at 15-30°C
- spin at 12,000 g for 15 min at 4°C

### RNA precipitation

- stain RNA by adding 1 µl GlycoBlue (15 mg/ml, Ambion Inc.) to a new RNase free Sarstedt tube.
- transfer the upper clear phase to the new RNase free Sarstedt tube.
- precipitate RNA by adding 500 µl isopropanol
- mix thoroughly by pipetting up and down
- incubate 10 min at 15-30°C
- spin down at 12,000 g for 10 min at 4°C

### Washing

- discard supernatant (carefully with small tips)
- add 500 µl 70% ethanol (1 ml/ml Trizol)
- spin down at 7,500 g for 5 min at 4°C
- discard supernatant carefully (use small tips)
- spin down (short)
- discard the remaining liquid

### Dilution of the RNA pellet

- dry pellet on air

- dilute RNA pellet in 30 µl nuclease free water (NFW)
- incubate 10 min at 55-60°C
- then chill on ice
- store RNA at -80°C

The absorbance at 260 nm and the A260/280 ratio of each sample was determined to measure RNA concentration and purity.

## 5.3 cDNA-Synthesis

### 5.3.1 TaqMan

cDNA synthesis was performed using the TaqMan MicroRNA Reverse Transcription Kit (applied biosystems) and a Thermocycler T3 (Biometra). See Table 3 for reaction mixture and cycle protocol.

(A) one reaction		(B) cycle protocol	
100mM dNTPs	0.10 µl	16°C	30 min
MultiScribe Reverse Transcriptase (RT) 50 U/µL	0.60 µl	42°C	30 min
10× Buffer	1.00 µl	85°C	5 min
RNase Inhibitor 20 U/µL	0.12 µl	4°C	pause
NFW	5.18 µl		
5× RT-Primer	2.00 µl		
RNA (10 ng)	1.00 µl		
total	10.00 µl		

**Table 3.** (A) reaction mixture for performing TaqMan-based cDNA synthesis, (B) cycle protocol thereof.

The following primers were used:

- U6b: RT 1093, RNU6B, 5x RT Primer (applied biosystems)
- miR-31: RT 1100, hsa miR-31, 5x RT Primer (applied biosystems)

### 5.3.2 Dynamo

For SYBR-Green-based qPCR, cDNA was synthesized by using the DyNAmo™ cDNA Synthesis Kit (Finnzymes). See Table 4Table 3 for reaction mixture and cycle protocol.

(A) one reaction	
Random Hexamers 300 ng/μl	1.00 μl
Reverse transcriptase	2.00 μl
2× RT buffer	10.00 μl
RNA (200 ng)	7.00 μl
total	20.00 μl

(B) cycle protocol	
25°C	10 min
37°C	30 min
85°C	5 min
4°C	pause

**Table 4.** (A) reaction mixture for performing DyNAmo™-based cDNA synthesis, (B) cycle protocol thereof.

## 5.4 qPCR

A threshold cycle (Ct) was defined within the exponential phase of the fluorescence signal of the qPCR. The Ct value of the target was subtracted by the Ct value of a housekeeping gene. The resulting dCt values were calculated as a fold change to a control sample ( $2^{-(dCt-dCt_{control})}$ ).

### 5.4.1 TaqMan

qPCR for microRNAs was performed using the TaqMan Universal PCR Master Mix, No AmpErase UNG (applied biosystems) and Rotor-Gene 6000 (Corbett Research). Data were analysed with Rotor-Gene 6.0 (Corbett Research). See Table 5 for reaction mixture and cycle protocol.

(A) one reaction	
Primer (20×)	0.5 μl
reaction buffer (2×)	5.0 μl
NFW	3.5 μl
template	1.0 μl
total	10.0 μl

(B) cycle protocol		
95°C	10 min	
95°C	10 sec	55x
60°C	45 sec	

**Table 5.** (A) reaction mixture for performing TaqMan-based qPCR, (B) cycle protocol thereof.

The following primers were used:

- U6b: TM 1093, RNU6B, 20x Real Time (applied biosystems)
- miR-31: TM 1100, hsa miR-31, 20x Real Time (applied biosystems)

Results of qPCRs for miR-31 were normalized to U6b.

### 5.4.2 Sensimix

qPCR for mRNAs was performed using the SensiMix™ SYBR & Fluorescein Kit (Bioline). See Table 6 for reaction mixture and cycle protocol. See Table 7 for primer sequences.

(A) one reaction	
Primer sense (10 pmol/μl)	0.25 μl
Primer antisense (10 pmol/μl)	0.25 μl
reaction buffer	5.00 μl
NFW	3.50 μl
cDNA	1.00 μl
total	10.00 μl

(B) cycle protocol		
95°C	10 min	
95°C	15 sec	55x
60°C	30 sec	
72°C	15 sec	
65-99°C	melting curve	

**Table 6.** (A) reaction mixture for performing Sensimix-based qPCR, (B) cycle protocol thereof.

BGLAP (Osteocalcin)	ATCAAAGAGGAGGGGAACCTA
	AGGAAGTAGGGTGCCATAACA
SPP1 (Osteopontin)	CACCTGTGCCATACCAGTTAAA
	AGCATCTGTGGGGCTAGG
Fzd-3	TGTCGTAGGCTGTGTCAGCGGGC
	TCTCTGCACTGCCACTGGGGCTC
GAPDH	CGACCACTTTGTCAAGCTCA
	TGTGAGGAGGGGAGATTCAG

**Table 7.** Primer sequences (forward and reverse) for four targets.

## 5.5 cell culture

### Passaging cells:

- for passaging HUVECs, the new Roux-flask needs to be coated before passaging: 3mL (T75) gelatine (1 % in PBS), incubate 10 min at 37°C. Remove excess gelatine and wash with PBS. HUVECs can now be passaged into the flask.
- remove medium from cells
- wash with PBS
- add trypsin 0.1 % + 0.02 % EDTA, incubate 5 min at 37°C
- check if cells are detached from flask wall
- add medium containing serum to inhibit trypsin
- resuspend cell suspension
- transfer cell suspension into new Roux-flask (take half of the present volume and add it to a Roux-flask of the same size for a 1:2 passage; PD (population doubling) increases by 1)
- add medium for a final volume of 6 mL (T25), 12 mL (T75) or 20 mL (T175)

## 5.6 Alizarin Red S staining

To detect calcification of AoSMCs cells were stained with Alizarin Red S which forms precipitates with calcium. Stained calcium deposits can be dissolved with HCl/SDS and can be measured colorimetrically.

- wash cells 3x with PBS (with Ca/Mg)
- fix cells at -20°C with 70 % ethanol (1-2h)
- wash 3x with AquaDest
- add Alizarin Red S (40 mM Alizarin Red S pH 4,2 – 0,14 g Alizarin Red S in 10 mL AquaDest, set pH with HCl) and shake 10min
- wash with PBS 10 min on shaker
- keep plates wet and take pictures
- add 500 µl 0,1 M HCl/0,5 % SDS, 30 min RT
- measure OD at 425 nm (take 150 µl for measurement in a 96-well-plate)

## 5.7 Calcification assay (high $\text{Ca}^{2+}/\text{P}_i$ )

AoSMCs, previously acquired from Lonza (referred to as 1<sup>st</sup> donor), were thawed at PD 8 and were cultured until PD 11 in growth medium consisting of SmGM-2 without the antibiotic GA-1000 (CC-3182, Lonza) and FBS (foetal bovine serum, final concentration 10 %).  $8 \times 10^4$  cells per well were seeded in growth medium (1 ml) in 12-well plates (Figure 5). Reverse transfection was done using siPORT Neo FX (applied biosystems). Cells were transfected with hsa-miR-31-precursor (AM17100) or pre-miR neg. ctr. 2 (Ambion) at a concentration of 30 mM according to the manufacturer's protocol. Transfection control was obtained 24 hours after transfection. To harvest cells, medium was removed, wells were washed with PBS and cells were treated with 0.5 ml 0.1 % Trypsin + 0.02 % EDTA for 5 – 10 min. 0.5 ml growth medium was then added and the cell suspension was transferred into an RNase/DNase free Sarstedt tube to further follow the RNA isolation protocol. 24 hours after seeding (referred to as day 1) the medium was changed to calcification medium (Dulbecco's Modified Eagle's Medium + 10 % FBS, 2.7 mM  $\text{CaCl}_2$ , 2.0 mM  $\text{NaH}_2\text{PO}_4$  based on an earlier report<sup>50</sup>) or control medium (DMEM + 10 % FBS) respectively. To measure calcification of cells, Alizarin Red S staining was performed on day 6 (plate 1) and on day 8 (plate 2). Pictures were taken before the Alizarin Red S staining was performed. To investigate intracellular levels of miR-31, cells were harvested on the same day as the Alizarin Red S staining. Cells which received calcification medium could not be detached by trypsinization. Therefore, cells were



harvested by directly adding Trizol to the well. RNA isolation, cDNA synthesis and qPCR were performed according to the given protocols. Results of qPCR were normalized to U6B.

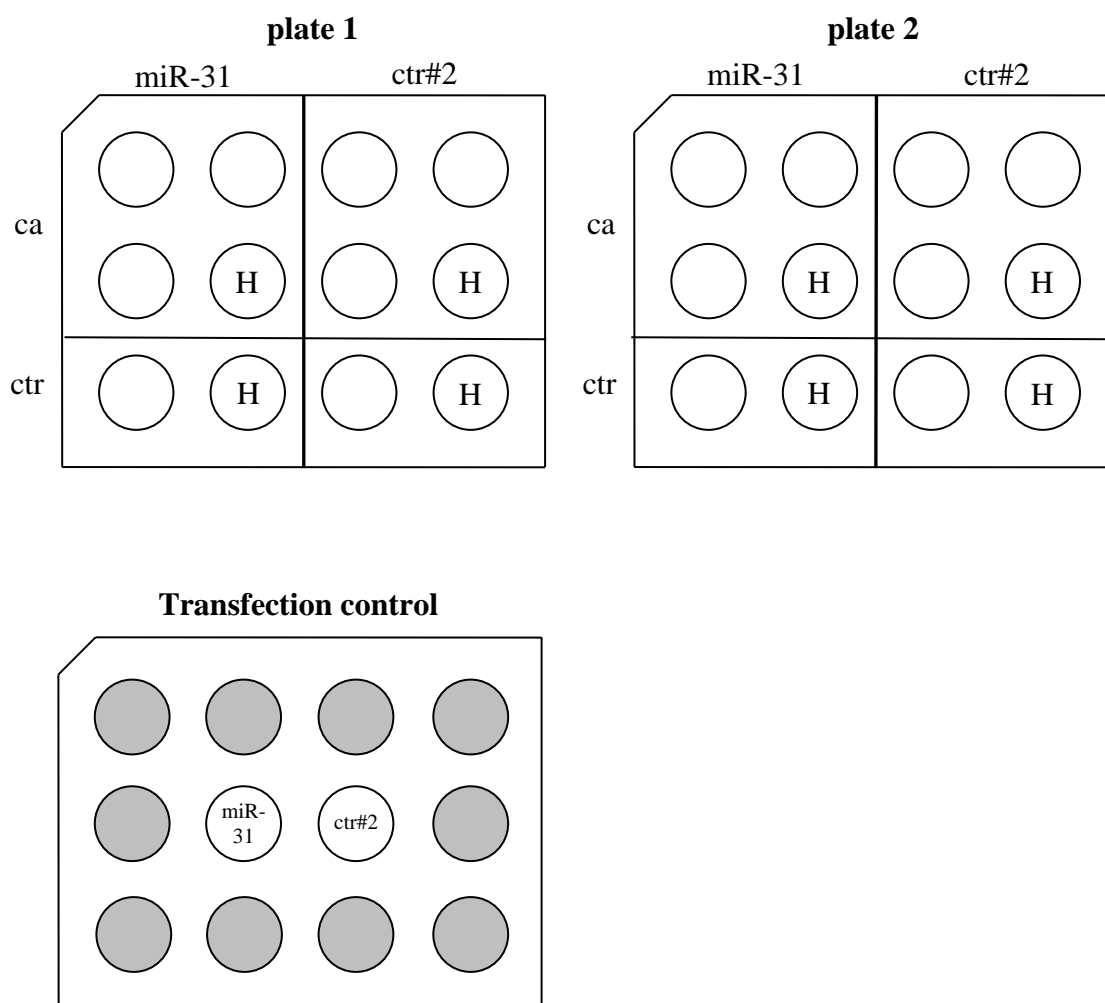


**Figure 5.** Plate design of the calcification assay. Three 12-well plates were used. Grey wells were filled with PBS. ca calcification media, ctr control media.

## 5.8 Calcification assay (low $\text{Ca}^{2+}/\text{P}_i$ ) – 1<sup>st</sup> donor

The assay was performed twice independently with AoSMCs from the same donor. For the first assay AoSMCs, previously acquired from Lonza (referred to as 1<sup>st</sup> donor), were thawed at PD 4 and were cultured until PD 8 in growth medium consisting of SmGM-2 without the antibiotic GA-1000 (CC-3182, Lonza) and FBS (final concentration 10 %). For the second assay AoSMCs were thawed at PD 6 and were cultured until PD 10.  $8 \times 10^4$  cells per well were seeded in growth medium (1 ml) in 12-well plates (Figure 6). Reverse transfection was done using siPORT Neo FX (applied biosystems). Cells were transfected either with hsa-miR-31-precursor (AM17100), pre-miR neg. ctr. 2 (Ambion), or siFzd3 (on target<sup>+</sup> smartpool,

Dharmacon, L-005502-00-0005) at a concentration of 30 mM according to the manufacturer's protocol. Transfection control was obtained 24 hours after transfection. To check transfection efficiency of siFzd3, cells were transfected with siGLO or siCTR and analysed by flow cytometry after 24 hours. To harvest cells, medium was removed, wells were washed with PBS and cells were treated with 0.5 ml 0.1 % Trypsin + 0.02 % EDTA for 5 – 10 min. 0.5 ml growth medium was then added and the cell suspension was transferred into an RNase/DNase free Sarstedt tube to further follow the RNA isolation protocol.

24 hours after seeding (referred to as day 1) the medium was changed to calcification medium (DMEM + 10 % FBS, 2.0 mM  $\text{CaCl}_2$ , 1.5 mM  $\text{NaH}_2\text{PO}_4$ ) or control medium (DMEM + 10 % FBS) respectively. Calcification of cells of the first assay was measured on day 7, the second assay on day 9. The measurement of calcification and the normalization to DNA content was performed according to the aforementioned protocol. Pictures were taken before adding 0.6 M HCl.

To investigate intracellular levels of miR-31 and mRNA levels of osteogenic markers, cells were harvested on the same day as the treatment for measuring the calcium concentration started. Cells which received calcification medium could not be detached by trypsinization. Therefore, calcifying and control cells were harvested by directly adding Trizol to the well. RNA isolation, cDNA synthesis and qPCR were performed according to the given protocols. U6B served as an internal control for qPCRs for miR-31. The level of osteogenic markers was normalized to GAPDH.

To combine the results of the two assays, the difference in calcification of miR-31 and ctr#2 transfected cells was calculated as a fold change to each value of the three control samples. We first calculated the mean of the resulting three fold changes per sample and then a mean of means of either miR-31 or ctr#2 transfected cells. Before analysing the statistical significance by student's t-test a log-transformation was applied to the fold changes.

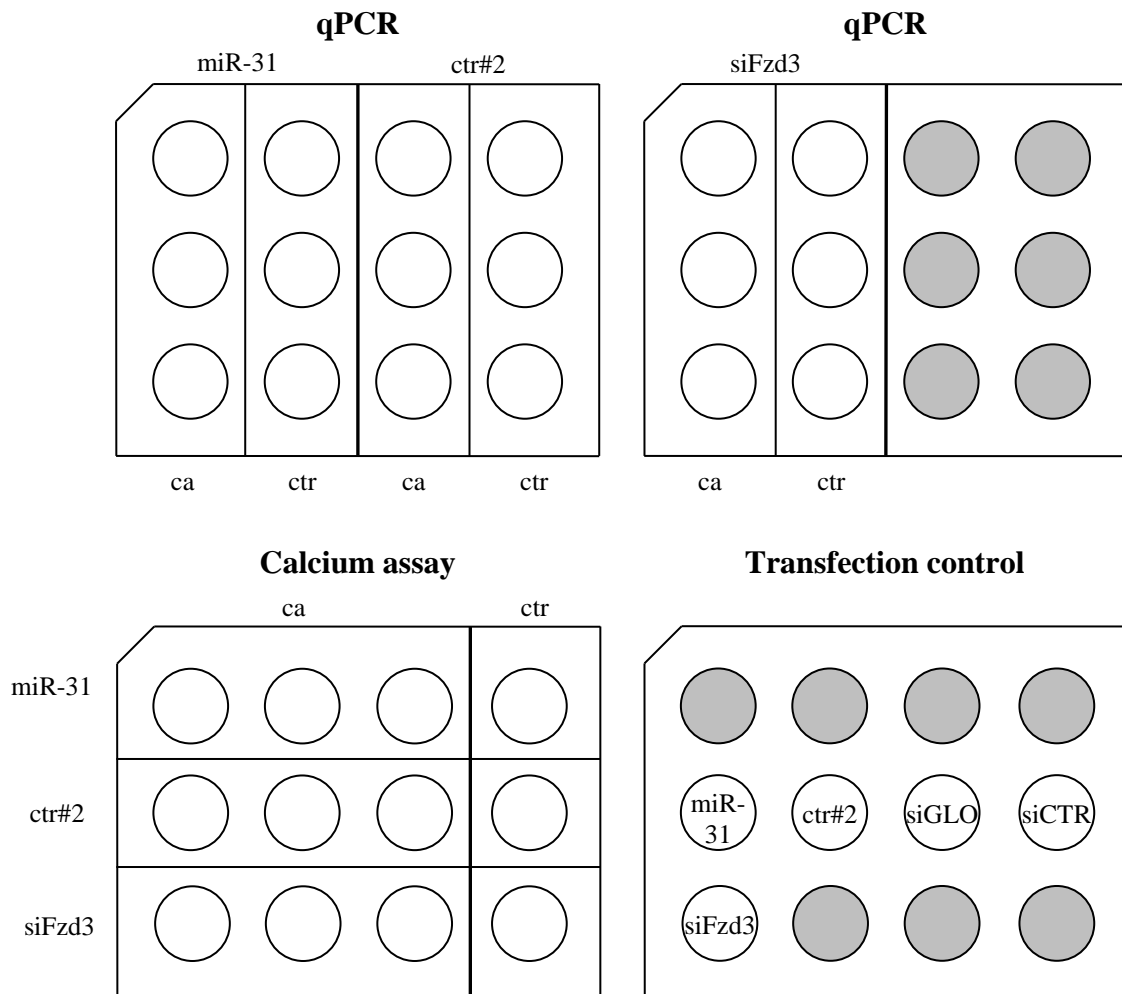


**Figure 6.** Plate design of the calcification assay. Four 12-well plates were used. Grey wells were filled with PBS. ca calcification media, ctr control media.

### 5.9 Calcification assay (low $\text{Ca}^{2+}/\text{P}_i$ ) – 2<sup>nd</sup> donor

The calcification assay performed with cells from the 1<sup>st</sup> donor was repeated with minor modifications. AoSMCs were acquired from the ATCC at PD 2. They were then cultured until PD 8 in growth medium consisting of SmGM-2 without the antibiotic GA-1000 (CC-3182, Lonza), 5% FBS, 10 mM L-glutamine and 50  $\mu\text{g}/\text{ml}$  L-ascorbic acid. Transfection with anti-miR-31 (Ambion, AM11465) was included (Figure 7). The differentiation was stopped at day 9, pictures were taken the same day.

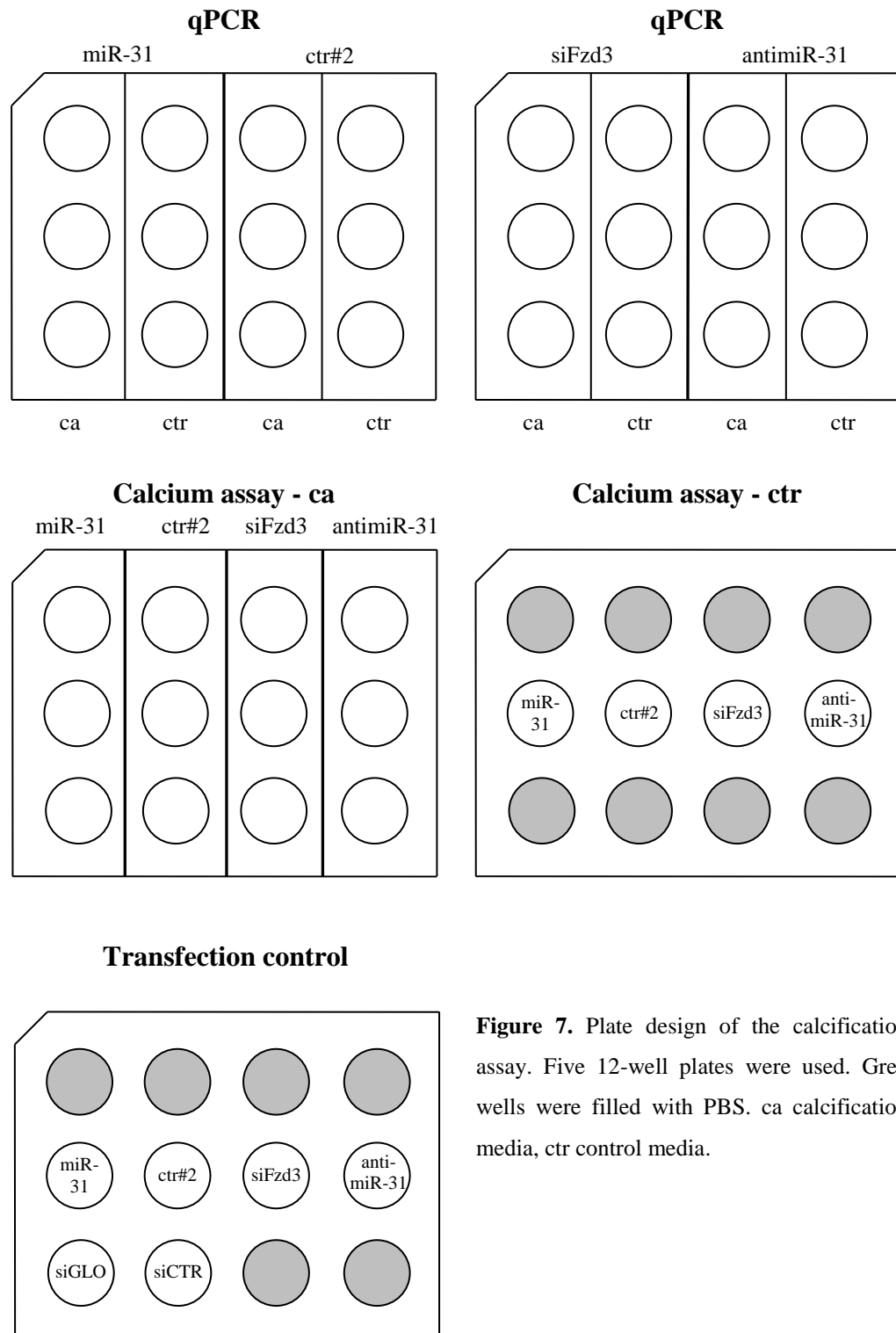


**Figure 7.** Plate design of the calcification assay. Five 12-well plates were used. Grey wells were filled with PBS. ca calcification media, ctr control media.

### 5.10 Long-term hydrocortisone treatment

HUVECs were cultured in EGM excluding the antibiotic GA-1000 (Lonza, CC-3124) and FBS (final concentration 10 %).  $10^5$  cells (PD 23) were seeded in a 6-well-plate and received either 2 ml culture medium free of HC or culture medium containing 2  $\mu$ M HC. Cells were

passed every 2 – 3 days. Medium was removed, wells were washed with PBS and cells were treated with 0.5 ml 0.1 % Trypsin + 0.02 % EDTA for 5 – 10 min. 0.5 ml culture medium was then added. Cell count was taken using a Bürker-Türk counting chamber. The same amount of cells (about half of the cell suspension) was seeded in every well of a new 6-well-plate. The other half of the cell suspension was transferred into an RNase/DNase free Sarstedt tube. Cells were spun down and 0.5 ml Trizol was added to the cell pellet for qPCR analysis of intracellular miR-31 levels. Results were normalized to U6b. To calculate the growth curve we assumed that cells grow on an infinite surface. The initially seeded cell count was multiplied by the growth rate of each passage.

### 5.11 Luciferase reporter plasmid

We used three different vectors to design the luciferase reporter plasmid (Figure 8): pCR2.1-TOPO (Invitrogen), pVAX1 (Invitrogen) to obtain a  $P_{cmv}$  promoter for the hPLALP gene (human placental alkaline phosphatase) and pMetLuc-Control (Clontech) for the secreted luciferase (Figure 38, appendix).

All gel and PCR clean-ups were performed using the Wizard® SV Gel and PCR Clean-Up System (Promega, A9281) according to the manufacturer's protocol. For minipreps we used Wizard® Plus SV Minipreps DNA Purification Systems (Promega, A1470).

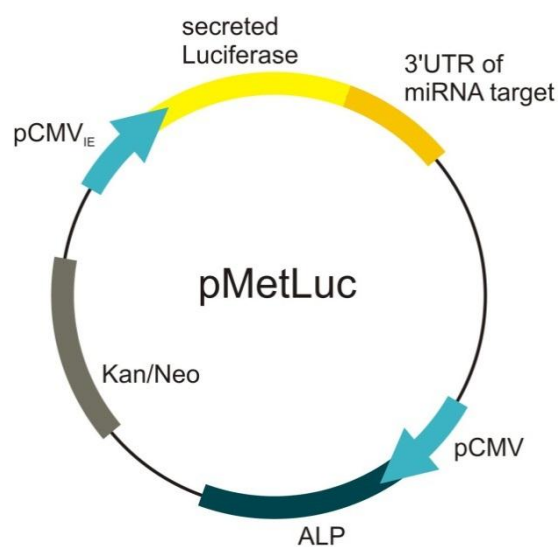


**Figure 8.** Luciferase reporter construct.

#### 5.11.1 DNA ladders

FastRuler™ High Range DNA Ladder, ready-to-use (Fermentas, SM1123)

Quantitas Fast DNA Marker: 100bp – 2kb (Biozym, 250224)

### 5.11.2 PCR

(A) reaction for hot TaqPol		(B) reaction for Phusion Pol	
dNTPs (10nM)	0.4 µl	dNTPs (10 nM)	0.4 µl
Primers (10 µM, sense + antis.)	2.0 µl	Primers (10 µM, sense + antis.)	2.0 µl
10× buffer	2.5 µl	5× HF buffer	4.0 µl
hot TaqPol (peqlab)	0.2 µl	Phusion Pol (Finnzymes)	0.2 µl
template (10 ng/µl)	1.0 µl	template (10 ng/µl)	1.0 µl
ddH <sub>2</sub> O	18.9 µl	ddH <sub>2</sub> O	12.4 µl
total	25.0 µl	total	20.0 µl

**Table 8.** reaction mixture for PCRs performed with either (A) hot TaqPol or (B) Phusion Pol

PCRs were performed either with either hot TaqPol or Phusion Pol. See Table 8 for reaction mixtures. Colony PCRs were performed by picking a colony from the plate and dissolving it in 20 µl LB medium. 1 µl of this medium served as a template. See Table 9 for cycle protocol used to amplify hPLALP out of Addgene plasmid 24595 (CMV-SEAP Amp<sup>R</sup>). Primer sequences used were:

- GCTAGCGCCACCATGCTGGGGCCCTGCAT (hPLALP\_NheI\_s)
- AATTGGGCCCACGCGCCGCAGCCA (hPLALP\_XbaI\_as)

cycle protocol		
98°C	30 sec	35 cycles
98°C	10 sec	
x <sub>1-8</sub> °C	30 sec	
72°C	10 min	
13°C	pause	

**Table 9.** Cycle protocol for amplifying hPLALP out of Addgene plasmid 24595 by PCR. x<sub>1-8</sub>: 55.9 – 58.0 – 60.4 – 62.8 – 65.2 – 67.6 – 69.9 – 72.1 °C

See Table 10 for cycle protocol used to amplify P<sub>CMV</sub>\_hPLALP out of pVAX1. Primers with restriction sites for ClaI:

- sense: ATCGATCGATGTACGGGCCAGATATACGC
- antisense: ATCGATTTCGCTTGCTGTCCATAAAACC

cycle protocol		
98°C	30 sec	
98°C	10 sec	35 cycles
72°C	81 sec	
72°C	10 min	
13°C	pause	

**Table 10.** Cycle protocol used for amplifying PCMV\_hPLALP out of pVAX1.

### 5.11.3 Addition of 3' A-overhangs

For cloning into the pCR2.1 vector 3' A-overhangs had to be added to the PCR products which were amplified by Phusion polymerase. The PCR product was run on a gel and the band was then cut out and cleaned up. See Table 11 for the exact protocol applied to the gel clean-up.

(A) reaction mixture	
Gel clean-up	21.3 µl
dATP [5 mM]	1.0 µl
10x Y buffer	2.5 µl
Taq Pol	0.2 µl

(B) temperature	
95°C	1 min
72°C	10 min
13°C	pause

**Table 11.** (A) reaction mixture and (B) temperature applied to add 3' A-overhangs.

### 5.11.4 Blue/White screening

1 plate	
IPTG [100 mM]	40 µl
XGal [50mg/ml]	32 µl
ddH <sub>2</sub> O	28 µl

**Table 12.** Treatment of one plate to enable blue/white screening

The pCR2.1 vector provided the possibility for blue/white screening to see if a colony is likely to contain the insert. See Table 12 for the solution with which one plate had to be treated before plating E. coli TOP10 transformed with pCR2.1

### 5.11.5 Ligation

For ligation with T4-Ligase the TA Cloning Kit (Invitrogen, K4500-01) was used with minor modifications. The reaction mixture was first incubated at 16°C for 1 hour and then at 4°C o/n.

### 5.11.6 Dephosphorylation

To dephosphorylate the vector, the amount of DNA ends in pmol needs to be determined. This depends on the amount of vector present in a given volume  $y$  and the length of the vector. For  $x$  pmol DNA ends,  $x$   $\mu$ l of ALP (diluted 1:100) has to be added. The exact equation is:  $x \mu\text{l ALP}_{1:100} + y \mu\text{l digested vector} + 4 \mu\text{l } 10\times \text{ buffer} + z \mu\text{l ddH}_2\text{O} = 40 \mu\text{l}$

The whole reaction needs to incubate for 30 min in a shaking incubator (37°C, 300 rpm). The same amount  $x$  of  $\text{ALP}_{1:100}$  is then added and the reaction is incubated another 30 min in a shaking incubator (37°C, 300 rpm).

### 5.11.7 Chemical transformation

20  $\mu$ l TOP10 competent cells were thawed from -80°C to 4°C and 5  $\mu$ l ligation reaction were added. After an incubation of 30 min on ice a heat shock at 42°C for 90 sec was applied. Cells were put back on ice for 2 min, 80  $\mu$ l SOC medium was added and cells were then put on a shaking incubator for 1 hour at 37 °C before they were plated.

### 5.11.8 Restriction digest

For restriction of DNA we used NheI, XbaI, BspHI, SmaI, ClaI and EcoRI FastDigest® restriction enzymes (Fermentas) according to the manufacturer's protocol.

## 5.12 Statistical analysis

To test the statistical significance of the data a student's t-test was performed. A p-value less than 0.05 was considered significant, a p-value less than 0.01 was considered highly significant. The data are shown as a mean  $\pm$  standard deviation.



## 6 Results

### 6.1 Establishment of an AoSMC calcification assay

#### 6.1.1 Calcification assay (high $\text{Ca}^{2+}/\text{P}_i$ )

To test the influence of miR-31 on the calcification of AoSMCs, cells were either transfected with miR-31 or control#2 (ctr#2). The assay was performed twice on two different 12-well-plates at the same time. A transfection control was obtained after 24h (Figure 9) which revealed a highly elevated intracellular level of miR-31 upon miR-31 transfection (77.7 fold). Cells received either calcification or control media. One plate was stained for calcium on day 6, the other on day 8 to measure the calcification at an early and at a late stage of differentiation. Calcification media clearly led to a stronger Alizarin Red S staining compared to cells in control media.

Both assays showed a difference in cell number depending on the transfection (as can be seen in the pictures of Figure 10). The cell count of miR-31 transfected cells was higher in number compared to ctr#2 transfected cells. The difference in cell count possibly distorts the data and shows higher calcification where more cells are present. Hence, we tried to determine the cell number for normalization. Alizarin Red S stained cells refrain from being counted as they dissolve when adding 0.1 M HCl/0.5 % SDS to quantify the staining. Therefore, we tried to count the cells harvested for qPCR analysis by using a Bürker-Türk counting chamber. However, calcified AoSMCs did not detach from the well by trypsin (neither 0.1% nor 0.25% trypsin). Determination of the cell count, thus, was not possible. Performing this assay clearly showed us the urgent need to normalize any quantification of calcification to the cell count or a comparable parameter and prompted us to develop an adequate normalization method (see chapter 6.1.3 Normalization by SYBR Green I).

Furthermore, in this first attempt of investigating the effect of miR-31 on calcifying AoSMCs, cells calcified strongly in a very short period of time causing two problems. First, the effect of miR-31 could be too weak to interfere with such a quick process. Second, it makes it difficult to identify the moment where a significant difference in calcification is detectable before calcium deposition runs into saturation in both transfection conditions. These challenges had to be addressed before continuing with another calcification assay.

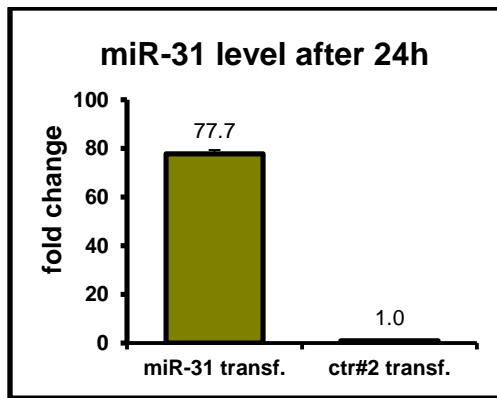


**Figure 9.** Transfection control taken 24 hours after transfection. Cells transfected (transf.) with miR-31 showed an increased level of miR-31 (77.7 fold) compared to cells transfected with ctr#2. Error bars indicate the standard deviation of the mean of quadruplets (technical replicates of the qPCR).

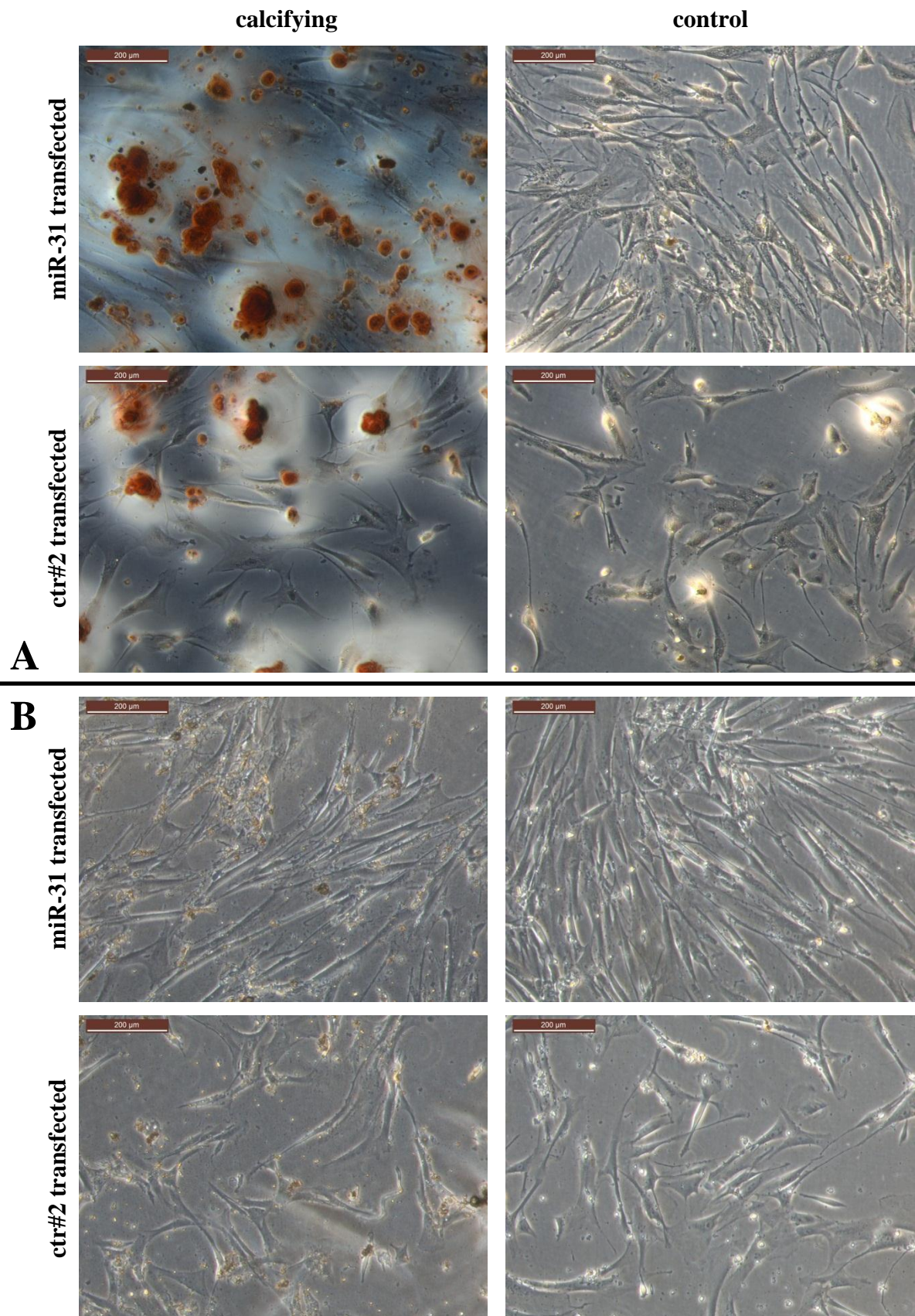
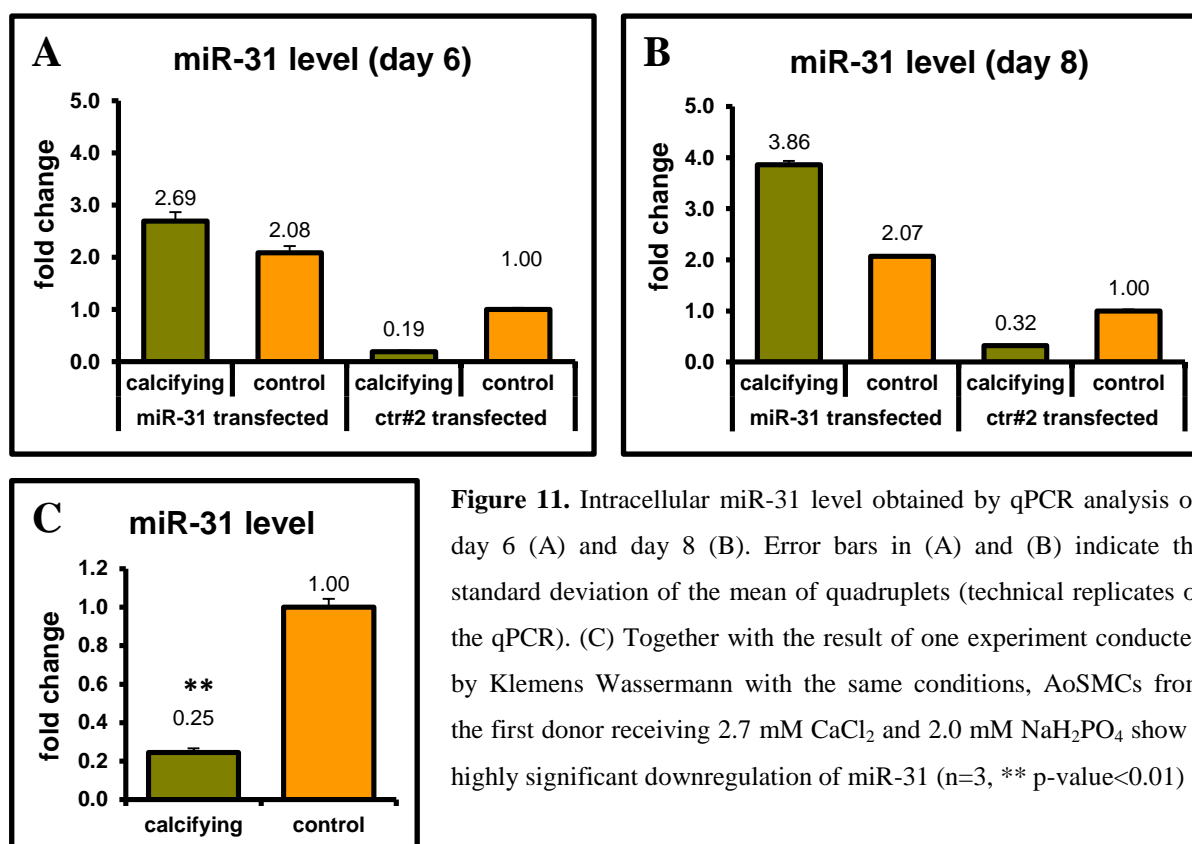


**Figure 10.** Pictures of AoSMCs in calcification or control media upon two different transfections taken (A) on day 6 after staining with Alizarin Red S and (B) on day 8 prior to the staining. A difference in cell count in favour of miR-31 transfected cells is clearly visible which possibly distorts any quantification results of the staining and prompted us to establish a method to normalize to DNA content.

On day 6 and 8, cells from one well of each condition were harvested for qPCR analysis (Figure 11A and B). miR-31 levels of miR-31 transfected cells were still elevated and ranged between 2 and 10 fold compared to ctr#2 transfected cells receiving the same media, proving that the transfection was effective enough to cover the whole time of the assay. In calcifying cells transfected with ctr#2, miR-31 was down-regulated between 3 and 5 fold. It should be noted that only one well per condition was harvested for qPCR. Nonetheless, together with a previous experiment done in our lab with the same conditions (Figure 11C) the present results provide strong evidence that miR-31 is down-regulated during the calcification process.



### 6.1.2 Optimization of calcification assay and monitoring miR-31 expression of AoSMCs over time

In the first calcification assay where we used a protocol kindly provided by Catherine Shanahan<sup>50</sup>, AoSMCs calcified strongly already after 6 days of incubation. Realizing that the calcification process might be too fast and calcium deposition might run into saturation we decided to test lower Ca<sup>2+</sup>/P<sub>i</sub> concentrations. The Ca<sup>2+</sup>/P<sub>i</sub> concentration used in the first calcification assay was included as a reference. An unusually high Ca<sup>2+</sup>/P<sub>i</sub> concentration was also tested to see its influence on intracellular miR-31 level. Cells were either stained with Alizarin Red S or harvested for investigating the miR-31 level by qPCR analysis.

The amount of calcification of AoSMCs was clearly dependent on the  $\text{Ca}^{2+}/\text{P}_i$  concentration in the differentiation media. As expected, AoSMCs receiving high  $\text{Ca}^{2+}/\text{P}_i$  stained strongly with Alizarin Red S already on day 7 of differentiation while  $\text{Ca}^{2+}/\text{P}_i$  concentrations ranging from 0.7/0.5 to 2.0/1.5 mM showed very little difference in calcification compared to cells receiving control media (Figure 12). Apparently there is a biological threshold within 2.0/1.5 and 2.7/2.0 mM  $\text{Ca}^{2+}/\text{P}_i$  over which AoSMCs show little resistance to calcification.

On day 9, however, cells receiving 2.0/1.5 mM  $\text{Ca}^{2+}/\text{P}_i$  have a more than 4-fold higher amount of calcification than cells in control media as can be seen in the inset of the graph of day 9 on Figure 12. This result convinced us to repeat the next calcification assay with media containing 2.0/1.5 mM  $\text{Ca}^{2+}/\text{P}_i$  and stopping it at around day 9.

The measurement of calcification at day 14 of AoSMCs receiving 8.1/6.0 mM  $\text{Ca}^{2+}/\text{P}_i$  could not be determined correctly. Due to the extraordinarily high amount of calcium deposits, the Alizarin-calcium-precipitates formed during the staining could not be extracted entirely by 0.1 M HCl/0.5 % SDS. Therefore the obtained OD value was too low and left out of the graph in order to avoid any misinterpretation.

To gain more evidence that miR-31 is down-regulated during calcification we had a look on the intracellular miR-31 level. Unfortunately, the obtained data by qPCR analysis did not give us a clear picture. The variation within the duplicates was considerable, in particular at day 7 for cells in control media or at day 9 across the board which makes it impossible to draw any substantial conclusions. Suspecting that the cDNA synthesis or qPCR did not work properly, both were repeated for the samples of day 9. Apart from one sample (0.7/0.5 mM  $\text{Ca}^{2+}/\text{P}_i$ ), the result of the second qPCR resembles the one of the first, showing high reproducibility of the assay (Figure 13).

At day 11 no substantial differences between the various conditions was observed except for the cells in media containing 8.1/6.0 mM  $\text{Ca}^{2+}/\text{P}_i$  which down-regulated miR-31 compared to cells in control media.



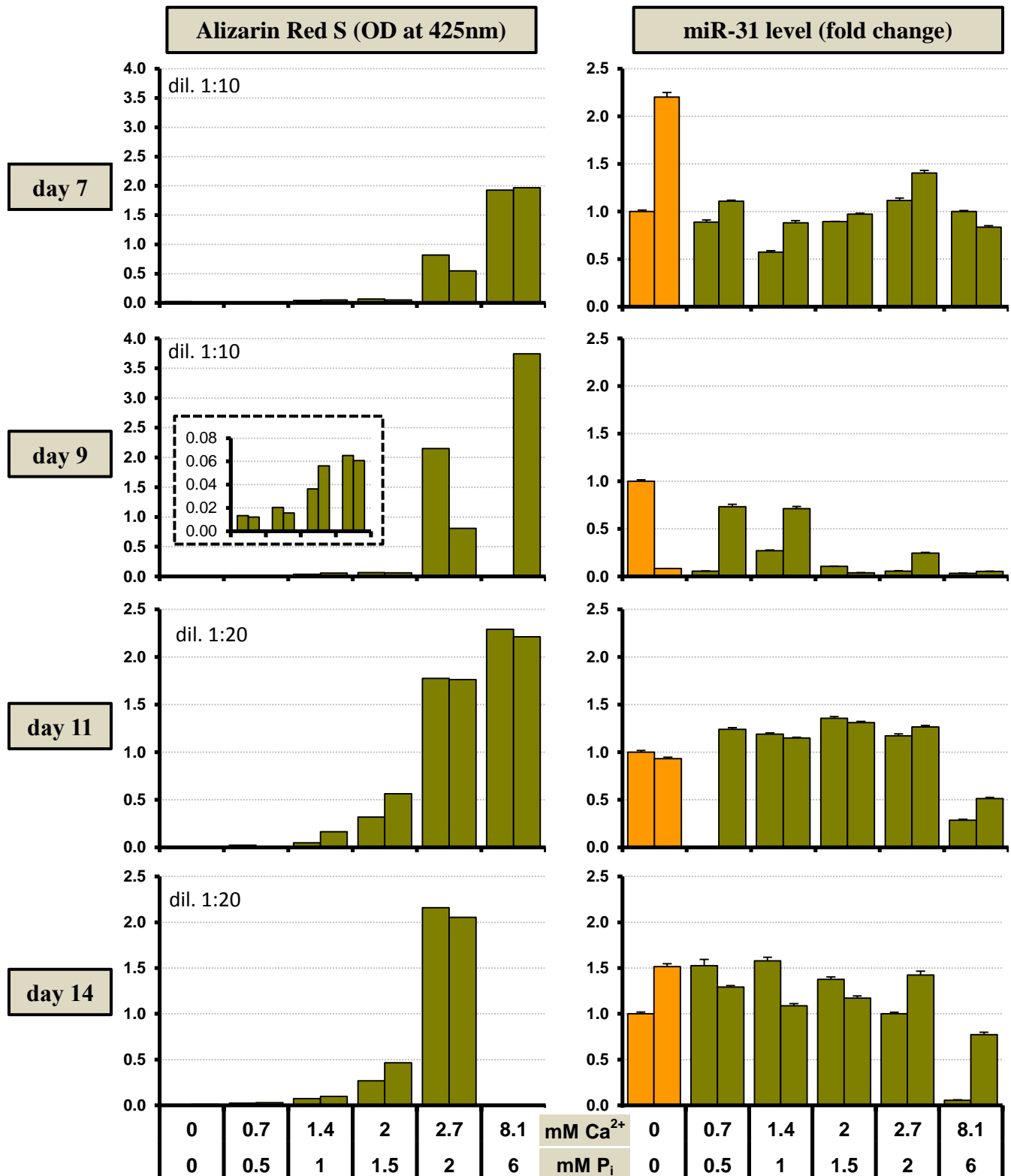


**Figure 12.** Calcification (left) and miR-31 level (right) measured at four different days in duplicates. The inset in the left graph of day 9 shows the Alizarin Red S readout of the four lowest  $\text{Ca}^{2+}/\text{P}_i$  concentrations. The dilution (dil.) of Alizarin Red S prior to reading is indicated in the graphs. Results of qPCR were normalized to the level of cells receiving 0/0  $\text{Ca}^{2+}/\text{P}_i$ . Error bars in the right graphs indicate the standard deviation of the mean of quadruplets (technical replicates of the qPCR). The label of the x-axis of the lowest graph applies to all of the above.

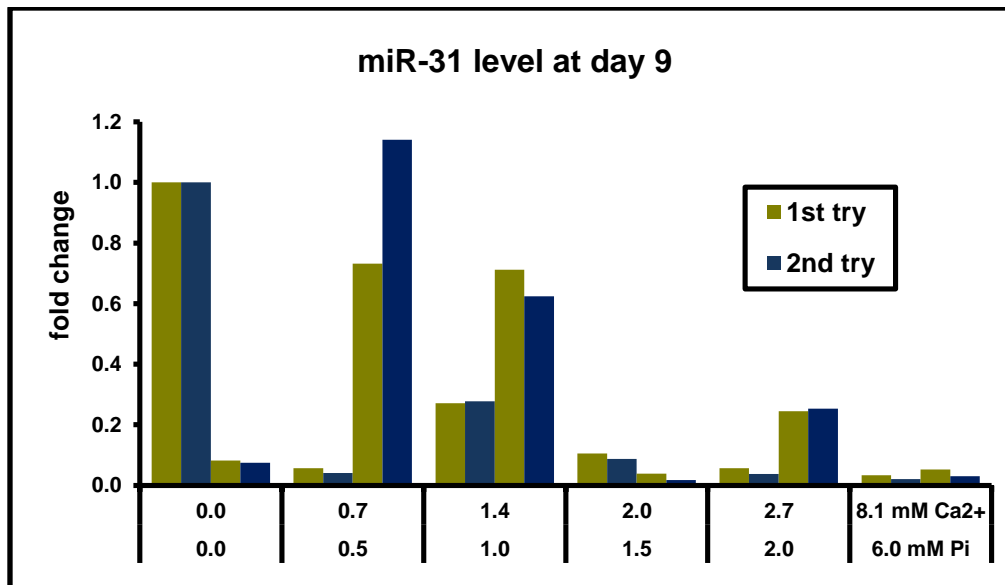


**Figure 13.** Result of two qPCRs from the same RNA samples, normalized to the level of cells receiving no Ca<sup>2+</sup>/P<sub>i</sub>.

### 6.1.3 Normalization by SYBR Green I

In order to normalize the amount of calcification to the cell number, cells were stained with SYBR Green I. The measurement of calcification as done in the first calcification assay (high Ca<sup>2+</sup>/P<sub>i</sub>) was changed and now included an overnight incubation with 0.6 M HCl. The incubation with HCl could hydrolyse DNA and hence make a DNA-based normalization inappropriate. To prove that this is not the case, various cell counts were seeded into 12-well plates and were treated with HCl as in the actual calcification assay. The number of cells correlates nicely with their FI caused by SYBR Green I staining ( $R^2 = 0.92$ , Figure 14) which makes it an ideal way to normalize the calcification to the cell count. We had a close look at the cells after the incubation with 0.6 M HCl to check if the AoSMCs' integrity and attachment to the well is not touched by the treatment. Pictures were taken before and after the overnight incubation in 0.6 M HCl. The cells remained in the well throughout the treatment (Figure 15).

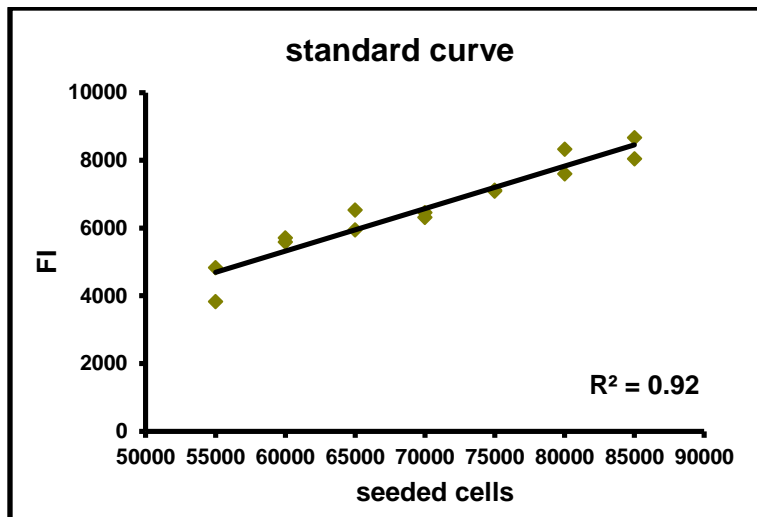


**Figure 14.** Standard curve for staining AoSMCs with SYBR Green I. Various cell counts were seeded in duplicates. FI Fluorescence Intensity.

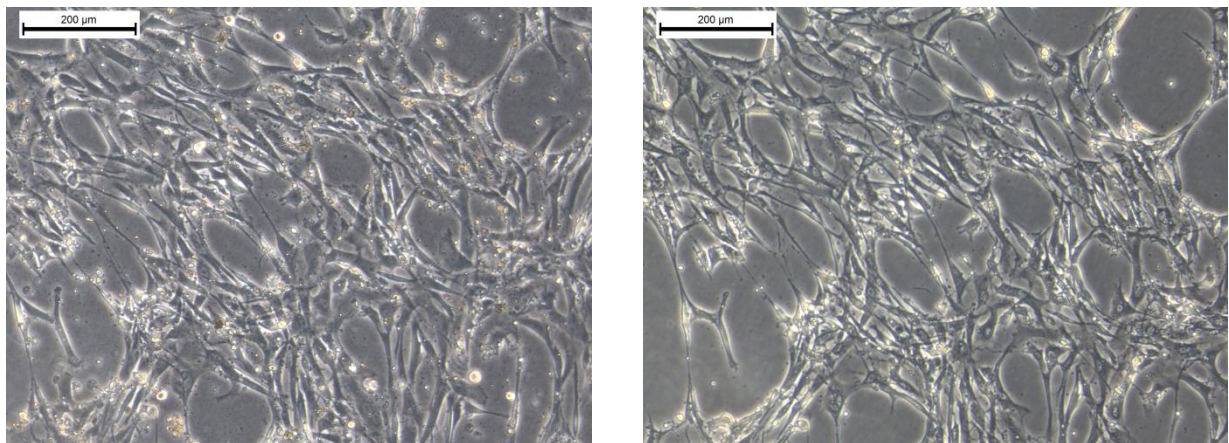


**Figure 15.** AoSMCs before (left) and after (right) incubation in 0.6 M HCl o/n at 4°C and washing with PBS. Cells stayed intact and did not detach from the well.

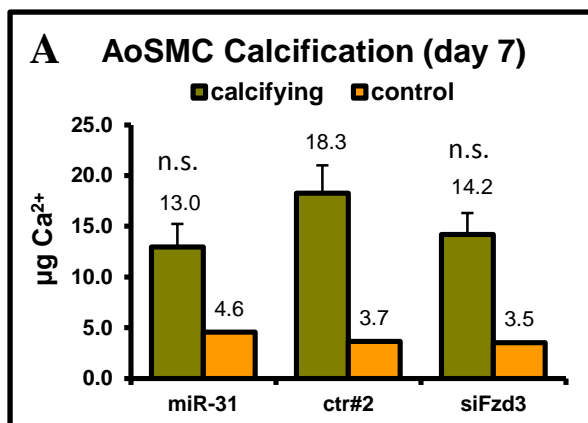
#### 6.1.4 Calcification assay (low $\text{Ca}^{2+}/\text{P}_i$ ) – 1<sup>st</sup> donor

The first calcification assay with a high concentration of  $\text{Ca}^{2+}/\text{P}_i$  clearly revealed some challenges. AoSMCs calcified too fast and the results of the Alizarin Red S staining could not be normalized to the number of cells. Therefore the concentration of  $\text{Ca}^{2+}/\text{P}_i$  in the differentiation media was lowered to 2.0/1.5 mM. The method for quantifying the calcification was changed as well. Instead of staining the cells with Alizarin Red S we determined the calcium content using the Quantichrom Calcium Assay kit (BioAssay Systems). After the decalcification of cells with 0.6 M HCl the cells remained attached to the well and we were able to perform the SYBR Green I staining. Results of the calcium measurement were normalized to the FI of the SYBR Green I staining.

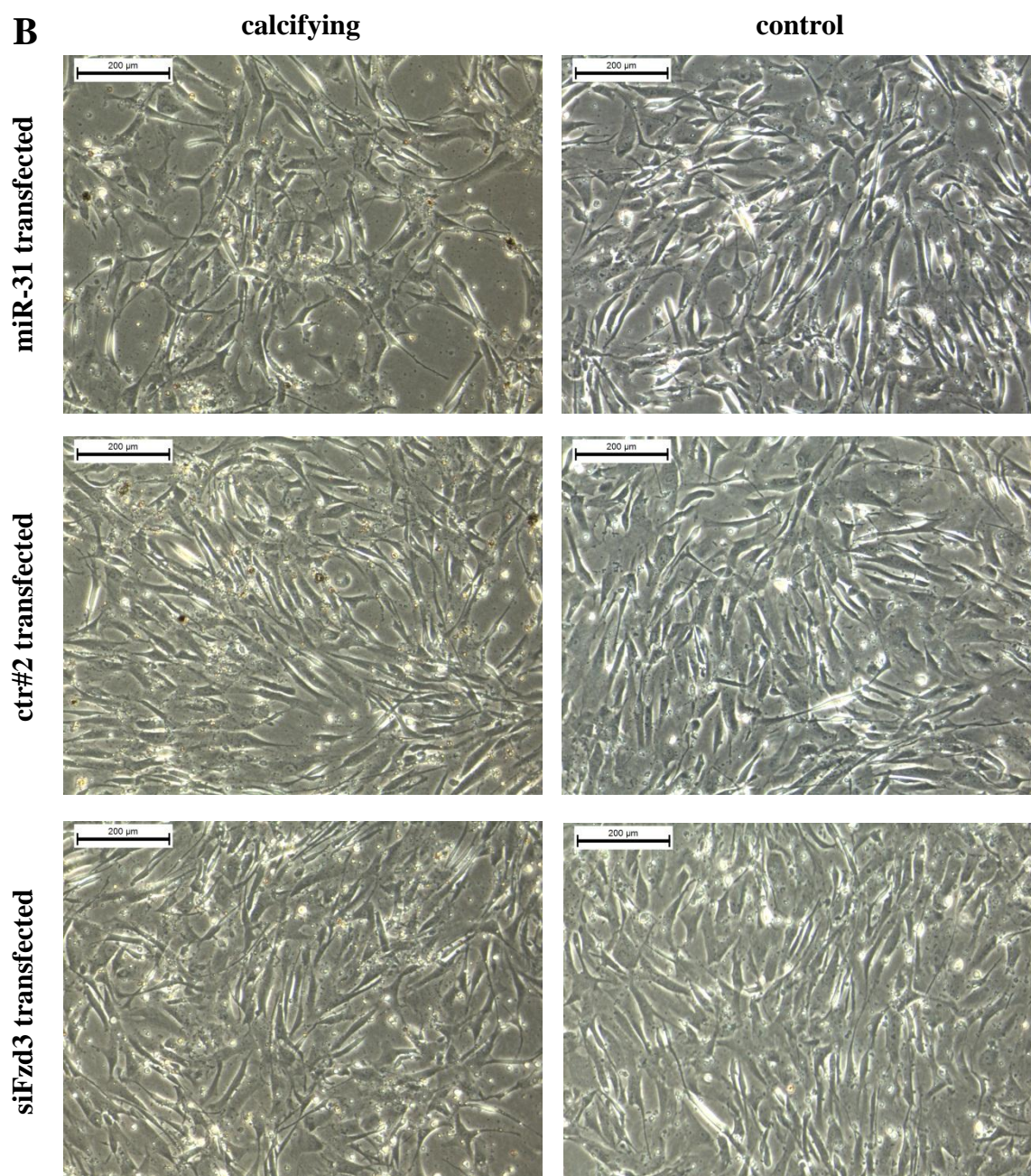


AoSMCs were transfected either with miR-31, control#2 or siFzd3. As mentioned earlier, Fzd3 is a confirmed target of miR-31<sup>60</sup>. The assay was performed twice independently and was stopped either at day 7 or at day 9 of differentiation. The transfection control taken 24 hours after transfection shows highly elevated intracellular miR-31 levels (between 850 and 1200 fold compared to ctr#2, Figure 19). In both assays miR-31 transfected cells in differentiation media were calcifying less than ctr#2 transfected cells, though the difference was not significant due to the high standard deviation within the triplicates (Figure 16A and Figure 17A). Cells transfected with siFzd3 calcified less than ctr#2 transfected cells only when looking at day 7 of differentiation but still the difference was not significant. The transfection itself did not seem to have an effect on the cell number which can be seen on the pictures of Figure 16B and Figure 17B. As in the calcification assay before, the cells did not proliferate throughout the experiment.

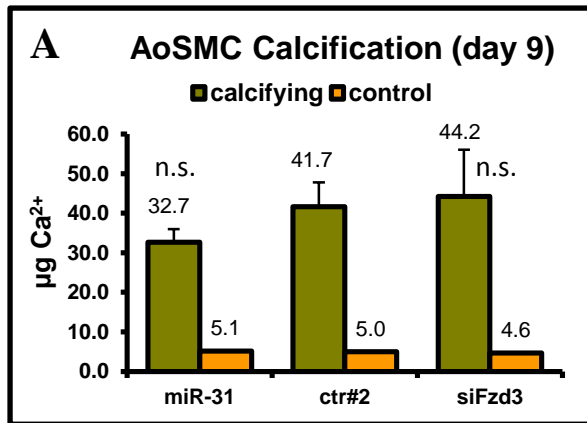
Taken the two experiments alone, miR-31 does not seem to have a significant effect on the AoSMCs' ability to calcify yet we see a clear trend towards miR-31 impeding this process. As mentioned above, the standard deviation of the triplicates is too high and was quite high in the assays performed before as well. To still prove significance the number of replicates had to be increased which we achieved by combining the two present assays performed with the same conditions and cells. The absolute amount of measured calcium differed between the two assays because they were stopped at two different days. Therefore, the difference in calcification was calculated as a fold change compared to ctr#2 transfected cells. The fold changes were then combined, a log-transformation was applied and a t-test was performed. AoSMCs were calcifying less by the amount of 25 % and this difference proved to be highly significant ( $P=0.004$ , Figure 18). As these in vitro data represent the reaction of only one donor, further evidence needs to be gained to prove the impeding effect of miR-31 on vascular calcification. First of all, more donors need to be included in the assay.



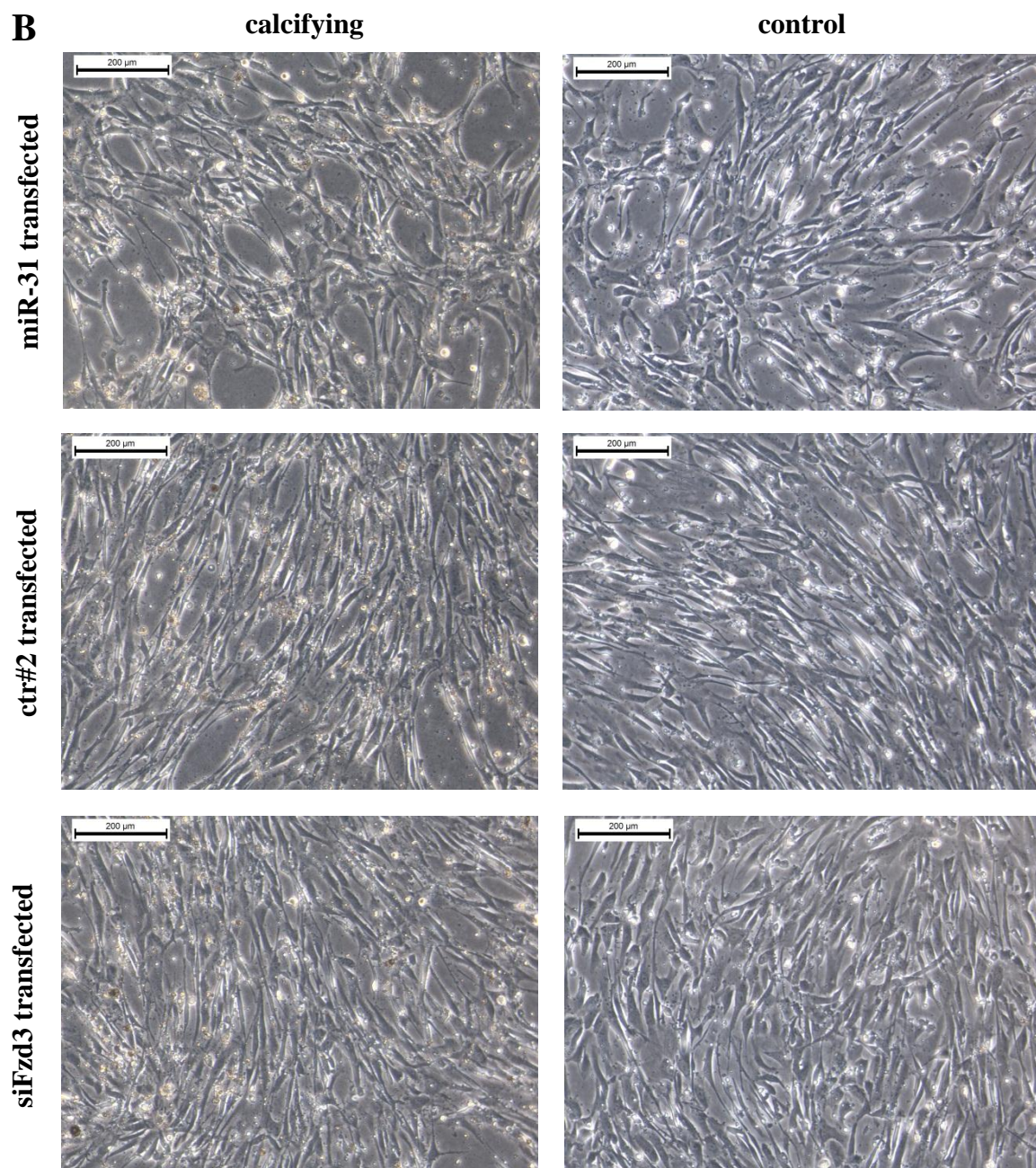
**Figure 16.** (A) Calcium content of cells after 6 days in differentiation or control media upon 3 different transfections. Error bars indicate the standard deviation of the mean of triplicates (n.s. not significant compared to ctr#2,  $P > 0.05$ ). (B) pictures taken at day 7 of differentiation.







**Figure 17.** (A) Calcium content of cells after 8 days in differentiation or control media upon 3 different transfections. Error bars indicate the standard deviation of the mean of triplicates (n.s. not significant compared to ctr#2,  $P > 0.05$ ). (B) pictures taken at day 9 of differentiation.



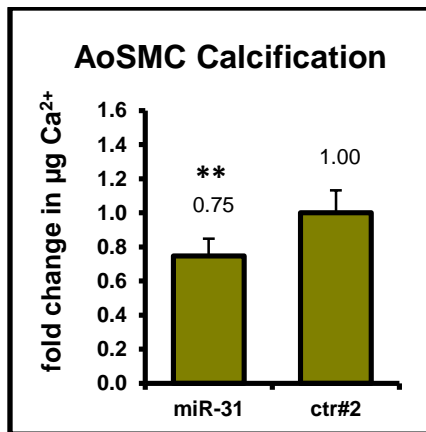


**Figure 18.** Fold change of calcification of AoSMCs when combining the two experiments to make the final number of replicates 6. (\*\* P = 0.004)

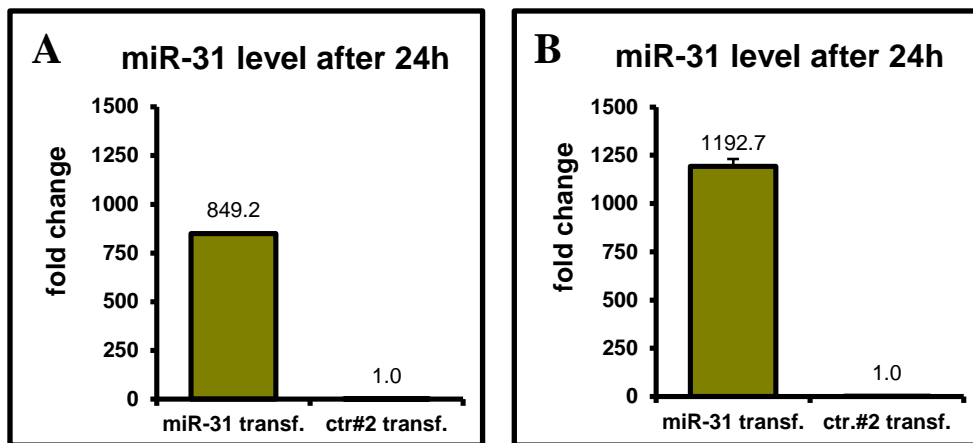


**Figure 19.** Transfection control taken 24 hours after transfection. The left graph (A) refers to the experiment stopped at day 7, the right one (B) to the experiment stopped at day 9. Error bars indicate the standard deviation of the mean of quadruplets (technical replicates of the qPCR).

As the transfection with miR-31 led to a weaker accumulation of calcium, we also investigated the mRNA levels of three osteogenic markers – osteocalcin (BGLAP), osteopontin (SPP1) and frizzled-3 (Fzd3). Osteocalcin is expressed by osteoblasts<sup>39</sup> and osteopontin is a reported inhibitor of calcification in vitro<sup>77</sup> and in vivo expressed by VSMCs<sup>78</sup>. Fzd3, as mentioned earlier, is a cell surface receptor that binds Wnt and is a confirmed target of miR-31<sup>60</sup>. Osteocalcin was not differentially regulated during the calcification of miR-31 or ctr#2 transfected cells (Figure 21), neither at day 7 nor at day 9. Therefore we did not have a look at the siFzd3 transfected cells. Osteopontin, however, proved to be up-regulated in cells receiving  $\text{Ca}^{2+}/\text{P}_i$  in the media. The difference in how much osteopontin is up-regulated in miR-31 and siFzd3 transfected cells is not significant compared to ctr#2 transfected cells. Regarding the assay which was stopped at day 9, miR-31 transfection led to a highly significant downregulation of osteopontin in AoSMCs receiving

control media but not in calcification media. Transfection with siFzd3 did not lead to any significant difference in osteopontin expression.

We did not observe any differential expression of Fzd3 at day 7 (Figure 21). The transfection control using siCTR/siGLO obtained after 24 hours showed a transfection efficiency of 41.7% and 63.6% for the assays stopped at day 7 and 9 respectively (Figure 20). Transfection with siFzd3 caused only a slight downregulation of Fzd3 in cells receiving control media. At day 9, however, Fzd3 was up-regulated in calcifying cells. AoSMCs transfected with miR-31 did not show a significantly lower upregulation of Fzd3 compared to ctr#2 transfected cells. siFzd3 transfected cells in control media have a significantly lower level of Fzd3 ( $P = 0.016$ ) and the transfection keeps Fzd3 down-regulated under osteogenic differentiation by 2.8-fold in comparison to calcifying ctr#2 transfected cells ( $P = 0.006$ ). We investigated two more markers for osteogenic differentiation, ALP and Runx2, in several samples but observed no differential expression (data not shown).

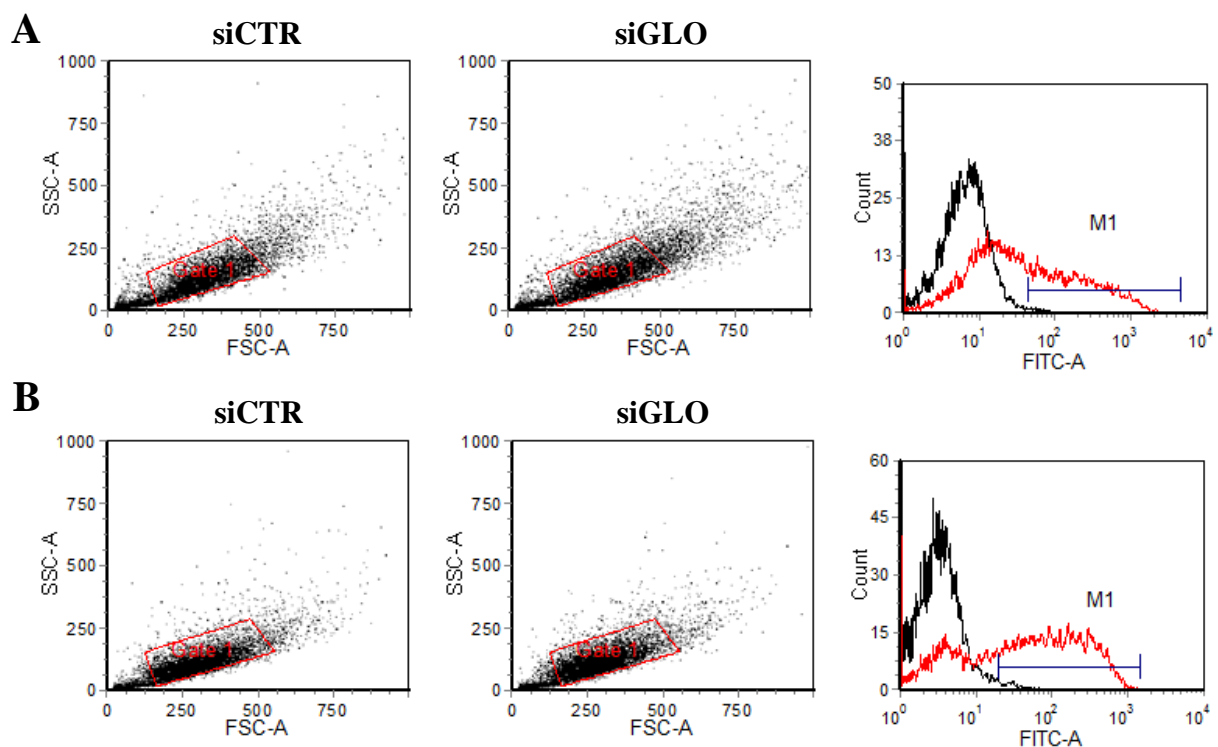


**Figure 20.** Cells transfected with siCTR and siGLO were analysed by FACS to estimate the transfection efficiency with siFzd3. Transfection efficiency was 41.7% (assay stopped at day 7, A) and 63.6% (assay stopped at day 9, B). Histogram: siCTR (black), siGLO (red).

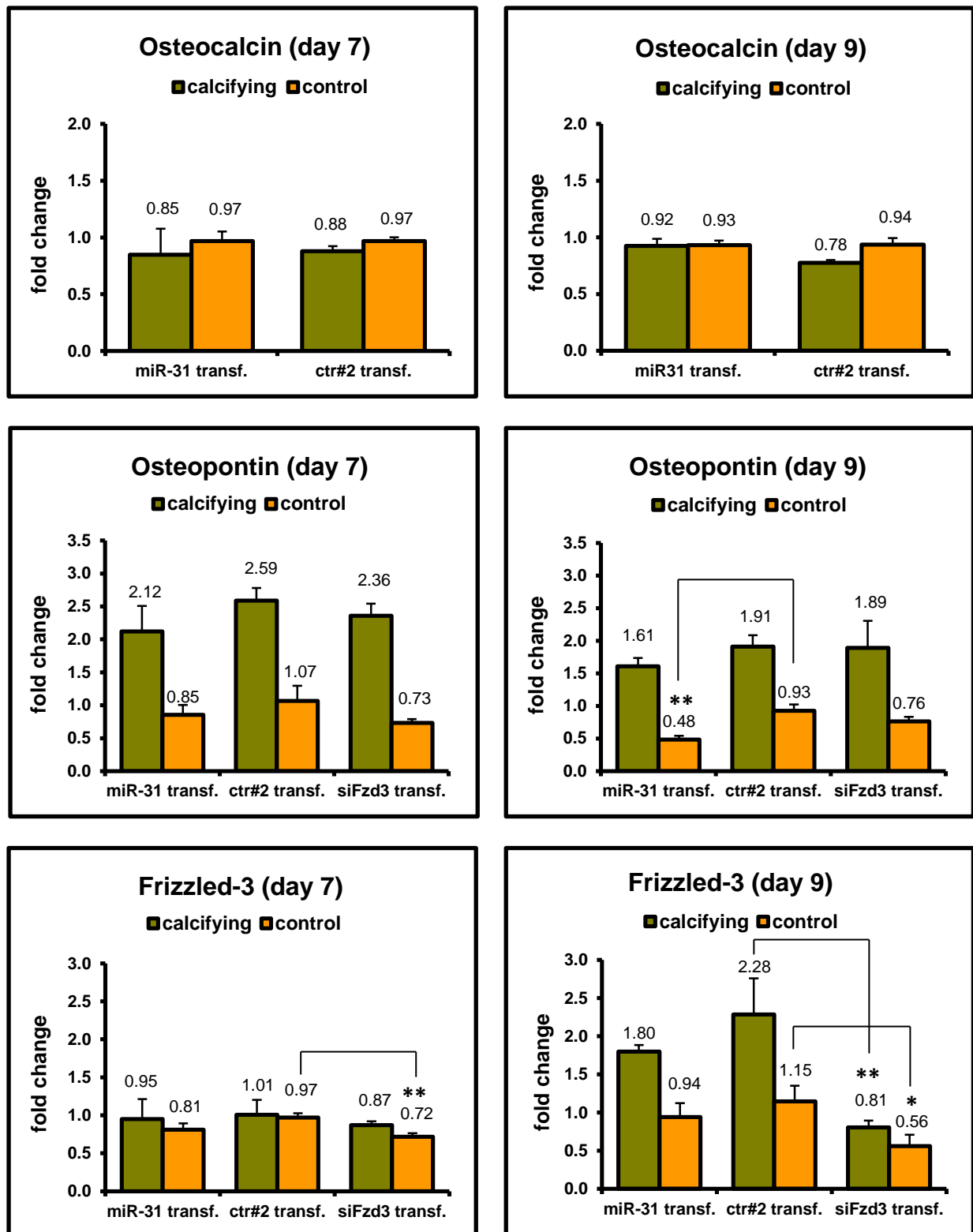


**Figure 21.** Results of qPCRs for three osteogenic markers at day 7 or day 9. Results are normalized to ctr#2 transfected cells receiving control media. Error bars show the standard deviation of the mean of triplicates. (\* P=0.02, \*\* P<0.01)



### 6.1.5 Calcification assay (low $\text{Ca}^{2+}/\text{P}_i$ ) – 2<sup>nd</sup> donor

Given that AoSMCs from the first donor responded to miR-31 transfection with weaker calcification, AoSMCs from another donor were acquired from the ATCC and we repeated the previous calcification assay. Transfection with antimiR-31 was included to see if it would contribute positively to the calcification.

In contrast to the first donor, miR-31 transfected AoSMCs from the second donor were calcifying significantly more than ctr#2 transfected cells ( $P = 0.04$ , Figure 22A). Transfection with antimiR-31, however, did not lead to the opposite effect and transfection with siFzd3 did not result in a significantly lower or higher amount of calcium as well.

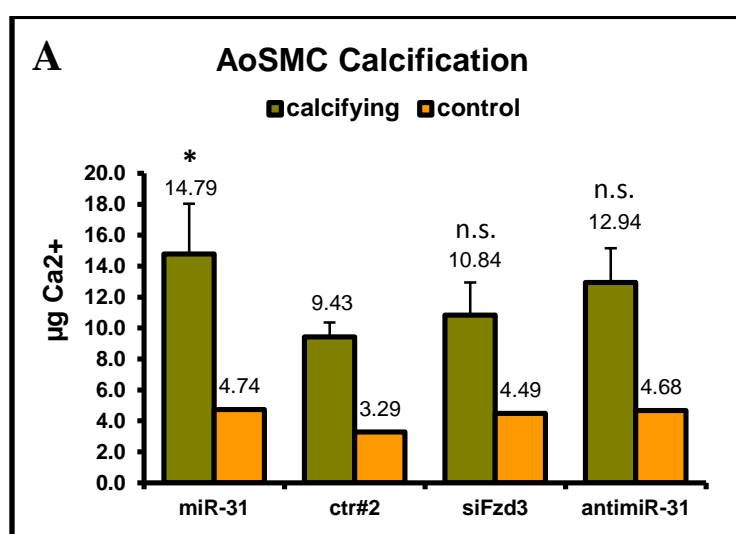
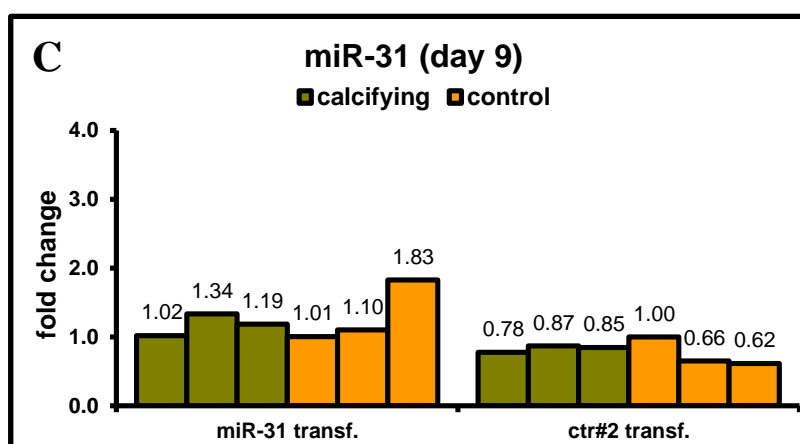
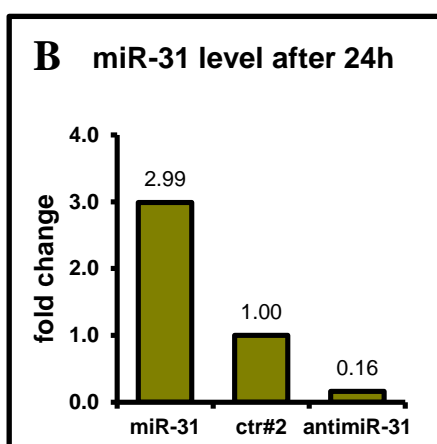


**Figure 22.** (A) Calcium content of cells after 8 days in differentiation or control media upon 4 different transfections. Error bars indicate the standard deviation of the mean of triplicates (n.s. not significant compared to calcifying ctr#2, \*  $P = 0.04$  compared to calcifying ctr#2). Transfection control taken 24 hours (B) and 9 days (C) after transfection showing low efficacy of transfection.



For transfection with miR-31, unfortunately, only a repeatedly frozen-thawed aliquot of miR-31-precursor was available. The resulting transfection was not successful as can be seen in the transfection control taken 24 hours after transfection (Figure 22B). Previous transfections resulted in a more than 800-fold higher miR-31 level compared to ctr#2 transfection (see Figure 19). The transfection in the present assay, though, resulted only in 3-fold higher miR-

31 level. Unsurprisingly, miR-31 levels were not elevated anymore at day 9 (Figure 22C). Transfection with anti-miR-31 caused a strong downregulation of the intracellular miR-31 level. The transfection control using siCTR/siGLO obtained after 24 hours showed a transfection efficiency of 52.0% (Figure 23).

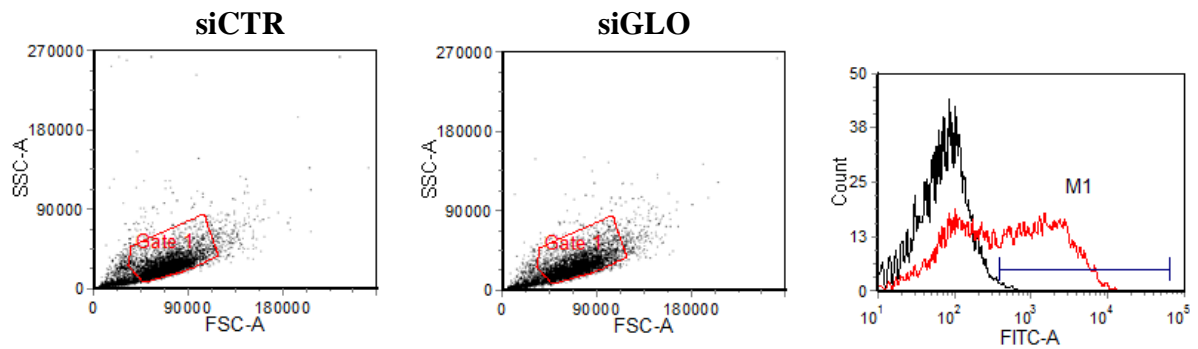


**Figure 23.** Cells transfected with siCTR and siGLO were analysed by FACS to estimate the transfection efficiency with siFzd3. Transfection efficiency was 52.0%. Histogram: siCTR (black), siGLO (red).

As opposed to the AoSMCs of the first donor, the cells of the second donor proliferated after transfection and change to differentiation/control media till they reached confluence which can be seen on the pictures of Figure 24, hence diluting the already weak transfection with miR-31.



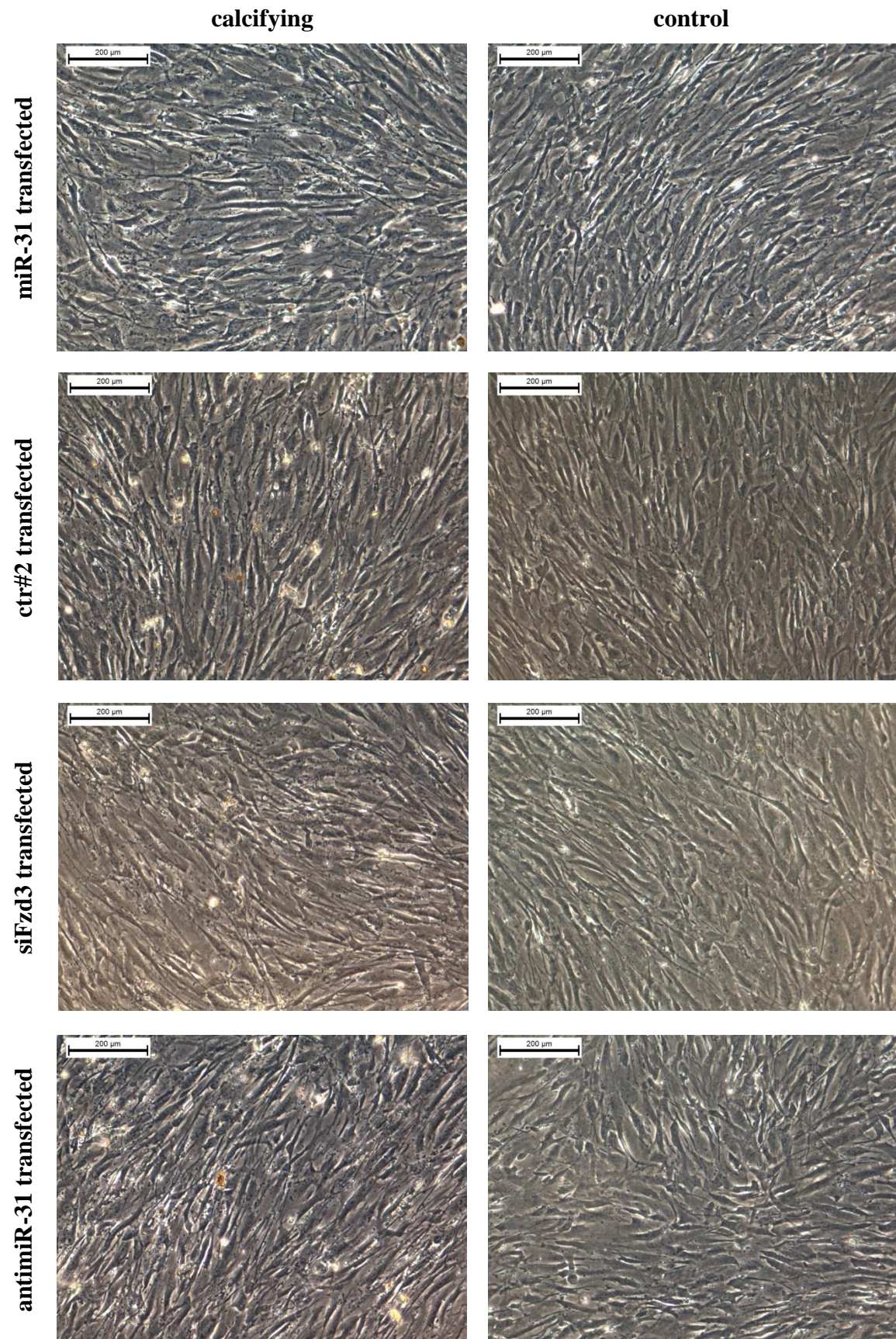


**Figure 24.** Pictures of AoSMCs from the 2<sup>nd</sup> donor taken at day 9 of differentiation.

## 6.2 Long-term hydrocortisone treatment

Previous short-term experiments showed an impact of HC on intracellular miR-31 level (data not shown). Treatment of HUVECs with 2  $\mu$ M HC for 24 hours led to an upregulation of miR-31 compared to cells receiving no HC. To elucidate the long-term effect of hydrocortisone, HUVECs were treated with 2  $\mu$ M HC for 5 passages. Before passaging, cells were counted and about half of the cells were harvested for qPCR analysis. In the beginning, we saw a trend that is consistent with our short-term experiments. The intracellular miR-31 level in the first passage seemed indeed higher in cells treated with HC but the trend turned after passaging the cells and resulted in HC-treated cells exhibiting a lower miR-31 level compared to the control (Figure 25). As seen in previous experiments where we determined the level of miR-31, the variation among the triplicates was again considerable and none of the differences discovered between cells receiving HC and the control were statistically significant. Previous attempts using duplicates delivered similar results (data not shown).

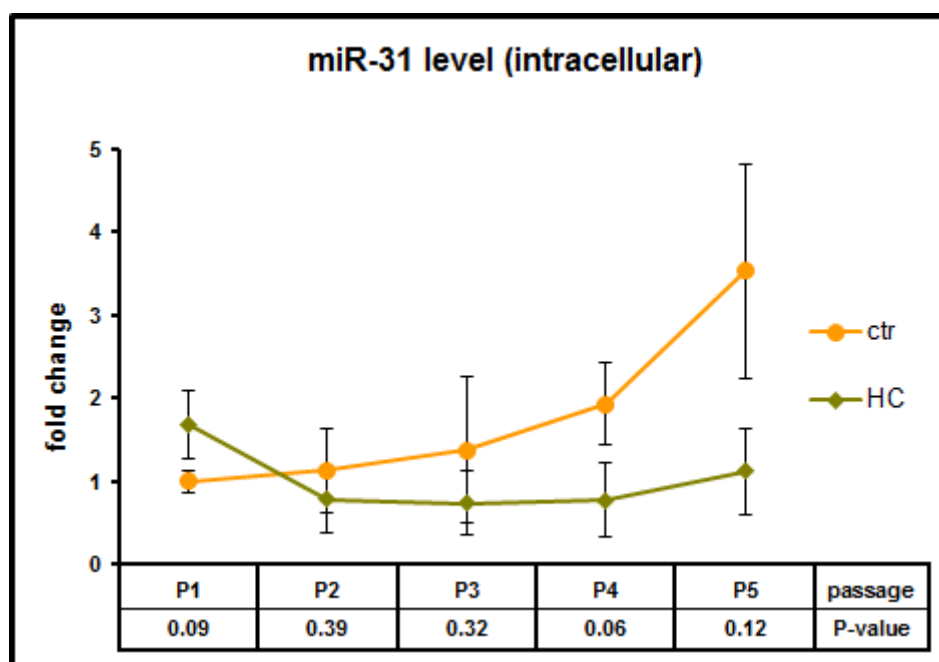


**Figure 25.** Result of qPCRs for intracellular miR-31 level in HUVECs treated with 2  $\mu$ M HC or no HC (ctr). Error bars indicate the standard deviation of the mean of triplicates. None of the differences in miR-31 level between cells receiving HC and the control of the same passage proved to be significant.

The cell count revealed a stronger proliferation of cells receiving no HC (Figure 26).



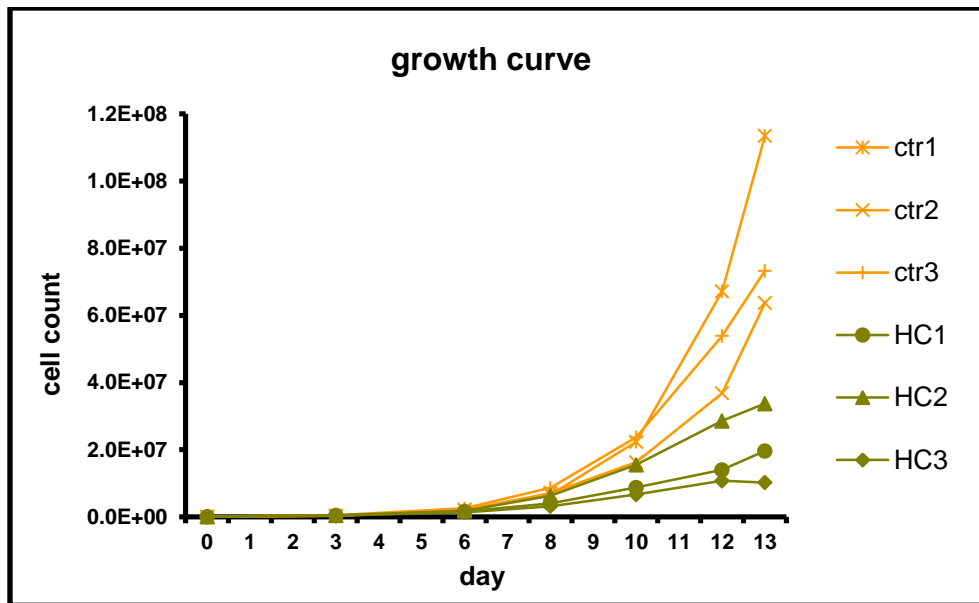


**Figure 26.** Cell count of HUVECs treated with 2  $\mu$ M HC or no HC (ctr).

### 6.3 Luciferase reporter plasmid

In order to determine further targets of miR-31 we attempted to design a luciferase reporter plasmid where the 3'UTR of putative targets can be cloned into and secretion of the luciferase could be normalized to the expression of a placental alkaline phosphatase. An o/n culture of *E. coli* TOP10 featuring the gene for human placental alkaline phosphatase (hPLALP, 1548 bp) was prepared (4 ml LB + 100  $\mu$ g/ml ampicillin). A miniprep was performed the next day followed by a PCR to amplify hPLALP using eight different annealing temperatures. Primers hPLALP\_XbaI\_as and hPLALP\_NheI\_s were used, the latter introducing a restriction sites for NheI. The PCR products were run on a 1% agarose gel (Figure 27). The upper bands on lane 6, 7 and 8 were excised and cleaned up.



**Figure 27.** 1% agarose gel. hPLALP (1548 bp) was amplified by PCR using eight different annealing temperatures.

3' A-overhangs were added to the amplified hPLALP by Taq Polymerase. The reaction product was cleaned up and 6  $\mu$ l were ligated with pCR2.1. TOP10 competent cells were transformed chemically with the ligation product and spread on an LB plate (100  $\mu$ g/ml ampicillin + XGal + IPTG for blue/white screening). 6 white colonies were checked for the

insert by colony PCR using primers hPLALP\_NheI\_s and hPLALP\_XbaI\_as. The PCR products were checked on a 1% agarose gel (Figure 28).



**Figure 28.** 1% agarose gel to check for amplification products of a colony PCR of 6 clones and a negative control (ddH<sub>2</sub>O)

Clones number 4 and 6 proved positive for the insert. Hence, o/n cultures of both were prepared in LB + Amp [100µg/ml]. A miniprep was performed the next day. Both minipreps were restricted with NheI/XbaI or BspHI to check the correct orientation of the insert. If correct, the resulting fragments of the BspHI restriction should be 3304 bp and 2173 bp long and the fragments after NheI/XbaI restriction should be 3879 bp and 1598 bp long. If falsely oriented, restriction with BspHI leads to a 3829 bp and a 1648 bp fragment and NheI/XbaI restriction results in two fragments of 5422 bp and 55 bp length. The reaction was then loaded onto a 1% agarose gel (Figure 29).

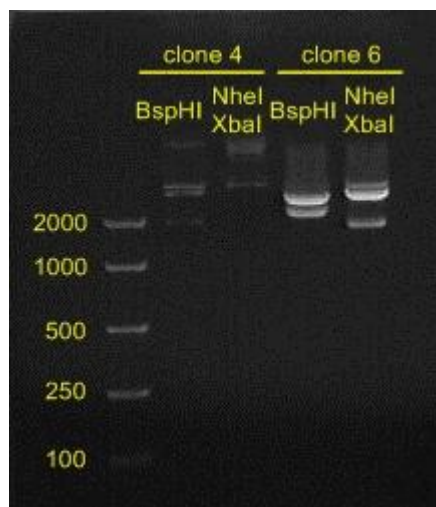


**Figure 29.** A restriction digest was loaded onto a 1% agarose gel to check if the hPLALP insert is oriented correctly in the pCR2.1 vector.

Clone number 6 proved to contain the hPLALP insert in the correct orientation. A glycerol stock of this clone was therefore stored at -80°C and the clone was sequenced. The sequencing result showed sufficient alignment with the gene hPLALP (>99%) with only one silent mutation. A miniprep of clone 6 and TOP10\_pVAX1 was restricted with NheI/XbaI. Unfortunately, the two restriction enzymes were chosen poorly as they produce complementary ends. This makes religation of the digested vector highly probable. Therefore, the vector pVAX1 was dephosphorylated after restriction. The restricted and dephosphorylated pVAX1, the restricted clone 6 containing hPLALP and a non-dephosphorylated pVAX1 as a control were loaded onto a 1% agarose gel (Figure 30).



**Figure 30.** 1% agarose gel showing the result of a restriction digest with *NheI/XbaI* of the vector pVAX1 and hPLALP. The vector was dephosphorylated (P-) after restriction.

hPLALP and the dephosphorylated pVAX1 were excised from the gel and cleaned up. After the ligation was performed, TOP10 were transformed and spread on LB-plates (30 µg/ml kanamycin). O/n cultures of 8 colonies were prepared and a miniprep was performed the following day. To check if the clones contain the plasmid with insert, the minipreps were digested with *SmaI* which cuts a 316 bp long fragment out of the insert.

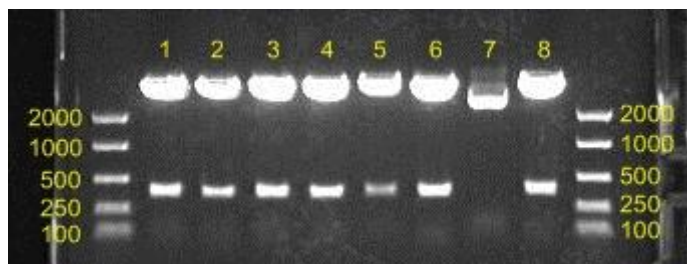


**Figure 31.** Restriction digest with *SmaI* on a 1% agarose gel to check 8 clones for the insert. If positive, *SmaI* cuts out a 316 bp long fragment.

Only clone number 7 did not contain the insert. The remaining seven were checked for correct orientation by digesting them with *NheI/XbaI*. The digestion only works if the insert is oriented correctly (Figure 32). Clones number 4 and 5 had the insert in the correct orientation.

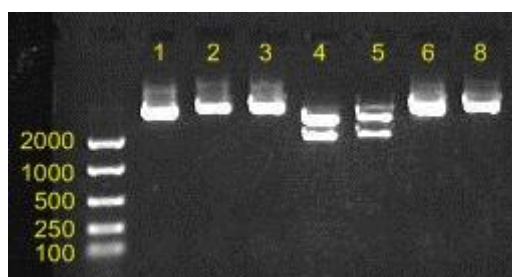


**Figure 32.** Restriction digest with *NheI/XbaI* on a 1% agarose gel to check for correct orientation of hPLALP in the vector pVAX1.

Minipreps of both clones were taken as a template for PCR with Phusion polymerase to amplify hPLALP together with a CMV promoter out of pVAX1. Primers for the PCR introduce a restriction site for *ClaI*. The PCR products were loaded on a 1% agarose gel (Figure 33). The expected size of P<sub>CMV</sub>-hPLALP is 2.6 kb.

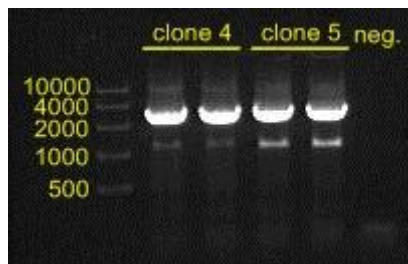


**Figure 33.** Products of a PCR for  $P_{CMV\_hPLALP}$  on pVAX1 loaded on a 1% agarose gel. The expected product length is 2.6 kb.

The bands of the appropriate size were cut out, cleaned up and a 3' A-overhang was added. The product was cleaned up again and ligated with pCR2.1. TOP10 cells were transformed with pCR2.1\_ $P_{CMV\_hPLALP}$  and spread on an LB plate containing kanamycin. A colony PCR with 8 white colonies was performed, the product was loaded on an agarose gel (Figure 34).



**Figure 34.** Result of a colony PCR for pCR2.1\_ $P_{CMV\_hPLALP}$  on a 1% agarose gel. 8 different clones were checked.

An o/n culture of clone number 1 and 6 was prepared. After performing a miniprep for both, the vector pMetLuc Control (4.6 kb) and pCR2.1\_ $P_{CMV\_hPLALP}$  of clone 1 were cut with ClaI, pMetLuc Control was dephosphorylated and loaded on an agarose gel (Figure 35).

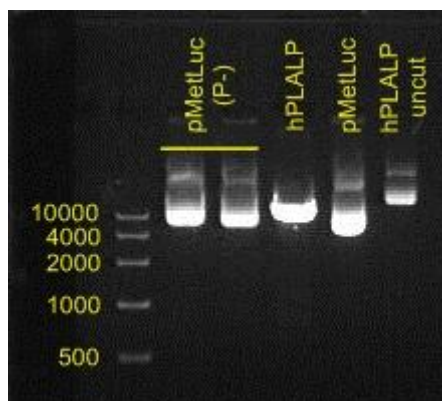


**Figure 35.** 1% agarose gel showing the dephosphorylated and ClaI digested vector pMetLuc(P-), ClaI digested pCR2.1\_ $P_{CMV\_hPLALP}$ , non-dephosphorylated pMetLuc and uncut pCR2.1\_ $P_{CMV\_hPLALP}$ .

Dephosphorylated pMetLuc Control was excised and cleaned up.  $P_{CMV\_hPLALP}$  was not cut by ClaI, hence the restriction digest was repeated together with a restriction digest with EcoRI to see if the insert may have changed (Figure 36). Not only could  $P_{CMV\_hPLALP}$  not be cut with ClaI but digestion with EcoRI also showed an additional band for both clones.

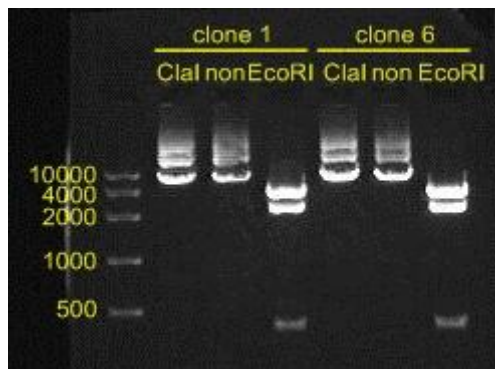


**Figure 36.** Restriction digest with ClaI, EcoRI or no restriction (non) of clones 1 and 6 on a 1% agarose gel.

Clones 2, 3 and 7 (referring to Figure 34) were checked as well by digesting them with ClaI. None of these clones could be restricted (Figure 37). Due to time constraints, the design of the luciferase reporter construct had to be stopped at this point and could not be finished.



**Figure 37.** Restriction digest with ClaI of clones number 2, 3 and 7 on a 1% agarose gel.

## 7 Discussion

### 7.1 miR-31 inhibits osteoblastic transition of VSMCs in one donor

CVDs are the main cause of death in the elderly population<sup>2</sup>. Atherosclerosis in particular accounts for most myocardial infarctions and stroke<sup>36</sup>. Mönckeberg's sclerosis contributes to arterial stiffness and is associated with widespread diseases like diabetes mellitus and chronic kidney disease<sup>26</sup>. In both atherosclerosis and Mönckeberg's sclerosis the arterial wall experiences calcification of VSMCs. It is now widely accepted that the calcification of VSMCs is a highly regulated process similar to bone calcification. There are a few miRNAs that have been established in the regulation of VSMCs so far. The miR-143/145-cluster, for instance, represses proliferation and promotes differentiation of VSMCs and is down-regulated in atherosclerosis<sup>59</sup>. Several miRNAs have been shown to regulate the differentiation of osteoblasts<sup>56</sup>. Based on our finding that miR-31 inhibits the differentiation of ASCs into osteoblasts we tested the hypothesis that miR-31 also inhibits the osteoblastic transition of VSMCs. Liu et al. recently described that rat miR-31 promotes proliferation of cultured VSMCs<sup>79</sup>. Given that proliferation and differentiation are often inversely related, miR-31 could indeed impede the osteogenic differentiation of VSMCs.

Our work on cultured human VSMCs supports this view. However, as we checked our hypothesis on VSMCs from only one donor successfully, its significance is limited. In order to properly investigate the effect of miR-31 on calcifying VSMCs we had to abolish our first attempt and changed the assay completely. The concentration of  $\text{Ca}^{2+}/\text{P}_i$  was too high and measuring the calcium content by Alizarin red S staining gave us no chance to normalize the result to the cell number or DNA content. After adjusting the assay we observed an inhibitory effect of miR-31 on the osteogenic differentiation (Figure 18). To determine the effect not only on calcium deposition but also on regulatory factors, we checked the mRNA levels of several osteogenic markers (Figure 21). Osteocalcin was not differentially regulated during osteogenic differentiation of VSMCs even though it is up-regulated in the differentiation of osteoblasts<sup>39</sup>. However, Nakano-Kurimoto et al. reported that osteocalcin is not elevated in senescent VSMCs undergoing osteoblast-like differentiation<sup>35</sup>. Our data suggests that the same is true for early-passage calcifying VSMCs. We also checked the mRNA level of osteopontin and observed a highly significant downregulation in miR-31 transfected VSMCs receiving control media. This suggests that miR-31 may interfere with osteogenic differentiation via inhibition of not only Fzd3 but also osteopontin or an upstream regulator. Transfection with miR-31 did not lead to a significant downregulation of Fzd3. Transfection



with siFzd3, however, led to a highly significant downregulation of Fzd3 at day 9 in both calcifying and control cells. Nonetheless, the successful transfection with siFzd3 did not result in weaker calcification at this time point. On the contrary, we did not observe a differential expression of Fzd3 regardless of the transfection. Still, we saw the inhibitory effect of miR-31 on calcification which suggests that Fzd3 cannot be the only target of miR-31 involved in osteogenic differentiation. A useful vector to investigate further targets of miR-31 would have been the luciferase reporter plasmid which remained unfinished due to time constraints. Similar reporter constructs were used previously to determine targets of miR-31<sup>60,62,68</sup>. Runx2 and ALP were not differentially regulated during VSMC calcification, neither at day 7 nor day 9. Zhu et al. demonstrated that also PiT-1, sclerostin, DMP-1 and E11 are up-regulated in calcifying VSMCs<sup>80</sup>. We plan to check for these markers and, since it is an early marker of osteogenic differentiation, for ALP at earlier time points in future experiments.

Furthermore, we asked if miR-31 is down-regulated during osteogenic differentiation of VSMCs as it was recently shown in human ASCs<sup>71</sup>. We saw this decline in miR-31 expression in the assay with high  $\text{Ca}^{2+}/\text{P}_i$  media (Figure 11A and B) and in a previous experiment done in our lab with the same conditions which leads to the conclusion that cells from the first donor significantly down-regulate miR-31 during the calcification process (Figure 11C). Monitoring the expression of miR-31 over time under different calcification media delivered inconsistent results with a considerable variation within duplicates (Figure 12). We were not able to repeat the assay with a higher number of replicates due to limited time and cell supply.

Repeating the calcification assay with VSMCs from a second donor was not successful because transfection with miR-31 failed (Figure 22B and C **Fehler! Verweisquelle konnte nicht gefunden werden.**) and the cells proliferated until they reached confluence which further diluted the weak transfection. The interpretation of the results of the second donor is, therefore, impossible. In this assay, the weak transfection with miR-31 led to a significantly higher amount of calcification compared to control cells (Figure 22). If the transfection had failed completely no difference in calcification should have been observed. If miR-31 indeed has a negative effect on the osteogenic differentiation of VSMCs anti-miR-31 should have the opposite effect. Unexpectedly, we observed no difference in calcification between anti-miR-31 transfected cells and control cells. As mentioned earlier, cells proliferated after the transfection which diluted its effect and makes it unclear if anti-miR-31 was effective throughout the assay. Additionally, VSMCs from the second donor were cultured in 5% FBS

instead of 10%. Nevertheless, the calcification assay was performed as done previously with 10% FBS. Liu et al. showed that FBS activates expression of miR-31<sup>79</sup>. Therefore, this switch in FBS concentration could have interfered with miR-31 expression, further distorting the results of this experiment.

As mentioned before, the significance of our work on calcifying VSMCs is so far limited due to the low number of donors. Nevertheless, there are several findings of other groups supporting our hypothesis. Similar to the putative effect of miR-31, miR-26a was demonstrated to inhibit osteogenic differentiation of human ASCs with its expression constantly increasing until reaching the highest expression level at osteogenic maturation<sup>81</sup>. miR-26a is also a crucial regulator of phenotype shifting of VSMCs, promoting proliferation while inhibiting differentiation<sup>59</sup>. A recently published study supports our hypothesis of an arterioprotective communication between senescent endothelial and smooth muscle cells via miRNAs<sup>82</sup>. Hergenreider et al. discovered that shear-stress-stimulated HUVECs secrete extracellular vesicles enriched in miR-143/145 which affects the gene expression of co-cultured smooth muscle cells. Application of these vesicles reduced the formation of atherosclerotic lesions in ApoE<sup>-/-</sup> mice.

Of course, there are a few findings opposing our view which should not remain unmentioned. BMP2 induces the differentiation of mesenchymal precursor cells into osteoblasts via activation of Runx2<sup>83</sup>. BMP2 was also shown to up-regulate miR-31 in mouse embryonic mesenchymal cells<sup>67</sup>. At first glance it seems contradictory that BMP2, a promoter of osteogenic differentiation, activates a putative inhibitor of VSMC calcification, miR-31. However, it is likely that activators of differentiation also induce expression of inhibitors as the process of differentiation requires fine-tuning and has to be stopped eventually. Moreover, it has been demonstrated in lung cancer cells that miR-31 targets Dkk-1<sup>62</sup>, an inhibitor of the Wnt signalling pathway. From this perspective one could consider miR-31 an activator of Wnt signalling and, thus, an activator of osteogenic differentiation. On the other hand, Fzd3, the aforementioned co-receptor binding to Wnt, is another target of miR-31<sup>60</sup>, demonstrating its negative interference at the very beginning of Wnt signalling. Generally, miRNAs target several mRNAs as well as one mRNA can be targeted by different miRNAs<sup>84</sup>. It is, hence, not unusual that miR-31 regulates different factors of the Wnt signalling pathway.

The ultimate goal of miRNA research in CVDs could be their establishment as biomarkers or therapeutic agents. Several miRNAs have been proposed to serve as biomarkers for CVDs like heart failure, coronary artery disease, diabetes mellitus or stroke. Circulating miRNAs

were found in secreted vesicles (microvesicles, exosomes, apoptotic bodies), protein-miRNA complexes or as by-products of dead cells<sup>85</sup>. A possible therapeutic effect of miRNAs could be harnessed by administration of antimiRs or the use of miRNA sponges which bind the miRNA of interest, making it no longer available for its targets. Also the upregulation of miRNAs could be of interest although this strategy had limited success so far<sup>86</sup>.

## **7.2 Investigating the role of hydrocortisone on the expression of miR-31 in HUVECs**

Glucocorticoids are commonly prescribed to treat diseases like rheumatoid arthritis or polymyalgia rheumatica. Long-term treatment with GCs such as hydrocortisone, however, leads to severe side effects like hypertension, insulin resistance or osteoporosis. 30% of patients develop osteoporosis when taking a GC for more than 6 months. This leads to bone loss and a higher risk of fractures<sup>72</sup>. GCs act on several factors involved in osteogenic differentiation, for instance type I collagen, osteocalcin or osteopontin<sup>73</sup>. Other groups as well as findings of ours established miR-31 as an inhibitor of osteogenic differentiation of ASCs. Furthermore, we found that endothelial cells secrete miR-31 in microvesicles, up-regulating miR-31 when undergoing senescence. We hypothesized that GCs act on endothelial cells by increasing their expression of miR-31 which further contributes to the development of cortisol-induced osteoporosis. Indeed, in short-term experiments we observed an upregulation of miR-31 in HUVECs incubated in media containing HC compared to HUVECs receiving no HC.

Here we tested the effect of HC treatment on HUVECs for 5 passages (Figure 25). The trend of the long-term experiment resembles the result of the short-term assay. While in the first passage miR-31 expression is higher in HC treated cells, values of HC and control cells level in the second passage. Control cells then start to increase expression of miR-31 compared to the first passage. Unfortunately, none of the differences between HC treated and control cells of the same passage is significant which makes a profound discussion of this data obsolete. Further experiments should include a marker sensitive to HC to check if the used concentration of 2µM is effective. Intriguingly, cells receiving no HC proliferated more (Figure 26) than cells receiving HC and seemed to have an increased level of miR-31 which raises the interesting question if miR-31 enhances proliferation not only in VSMCs<sup>79</sup> but also in endothelial cells. It remains elusive why the measured values for miR-31 are varying considerably among the triplicates which caused a high standard deviation and statistical insignificance. As discussed above, we observed this also in one of our calcification assays.

## 8 Acknowledgements

I would like to thank all the group members of the Grillarilabs at BOKU (University of Natural Resources and Life Sciences, Vienna) where I conducted most of my experiments, especially my supervisor Johannes Grillari and my tutor Klemens Wassermann as wells as my tutor Georg Feichtinger from the Ludwig Boltzmann Institute for Experimental and Clinical Traumatology where I started the design of the luciferase reporter plasmid. Thank you all for your kind help!

## 9 References

1. Kirkwood, T. B. & Austad, S. N. Why do we age? *Nature* **408**, 233–238 (2000).
2. Buchow, H., Cayotte, E. & Agafitei, L. Circulatory diseases - Main causes of death for persons aged 65 and more in Europe, 2009. *eurostat - Statistics in focus* (2012).
3. Murphy, W. A., Jr, Nedden Dz, D. zur, Gostner, P., Knapp, R., Recheis, W. & Seidler, H. The iceman: discovery and imaging. *Radiology* **226**, 614–629 (2003).
4. Campisi, J. & d' Adda di Fagagna, F. Cellular senescence: when bad things happen to good cells. *Nat. Rev. Mol. Cell Biol.* **8**, 729–740 (2007).
5. Kuilman, T., Michaloglou, C., Mooi, W. J. & Peeper, D. S. The essence of senescence. *Genes Dev.* **24**, 2463–2479 (2010).
6. Dimri, G. P., Lee, X., Basile, G., Acosta, M., Scott, G., Roskelley, C., Medrano, E. E., Linskens, M., Rubelj, I. & Pereira-Smith, O. A biomarker that identifies senescent human cells in culture and in aging skin in vivo. *Proc. Natl. Acad. Sci. U.S.A.* **92**, 9363–9367 (1995).
7. HAYFLICK, L. & MOORHEAD, P. S. The serial cultivation of human diploid cell strains. *Exp. Cell Res.* **25**, 585–621 (1961).
8. d' Adda di Fagagna, F. Living on a break: cellular senescence as a DNA-damage response. *Nat. Rev. Cancer* **8**, 512–522 (2008).
9. Collins, K. & Mitchell, J. R. Telomerase in the human organism. *Oncogene* **21**, 564–579 (2002).
10. Masutomi, K., Yu, E. Y., Khurts, S., Ben-Porath, I., Currier, J. L., Metz, G. B., Brooks, M. W., Kaneko, S., Murakami, S., DeCaprio, J. A., Weinberg, R. A., Stewart, S. A. & Hahn, W. C. Telomerase maintains telomere structure in normal human cells. *Cell* **114**, 241–253 (2003).
11. Rodier, F. & Campisi, J. Four faces of cellular senescence. *J. Cell Biol.* **192**, 547–556 (2011).
12. Serrano, M., Lin, A. W., McCurrach, M. E., Beach, D. & Lowe, S. W. Oncogenic ras provokes premature cell senescence associated with accumulation of p53 and p16INK4a. *Cell* **88**, 593–602 (1997).
13. Campisi, J. Cellular senescence: putting the paradoxes in perspective. *Curr. Opin. Genet. Dev.* **21**, 107–112 (2011).
14. Jaskelioff, M., Muller, F. L., Paik, J.-H., Thomas, E., Jiang, S., Adams, A. C., Sahin, E., Kost-Alimova, M., Protopopov, A., Cadiñanos, J., Horner, J. W., Maratos-Flier, E. & Depinho, R. A. Telomerase reactivation reverses tissue degeneration in aged telomerase-deficient mice. *Nature* **469**, 102–106 (2011).

15. Baker, D. J., Wijshake, T., Tchkonian, T., LeBrasseur, N. K., Childs, B. G., van de Sluis, B., Kirkland, J. L. & van Deursen, J. M. Clearance of p16Ink4a-positive senescent cells delays ageing-associated disorders. *Nature* **479**, 232–236 (2011).
16. Bernardes de Jesus, B., Vera, E., Schneeberger, K., Tejera, A. M., Ayuso, E., Bosch, F. & Blasco, M. A. Telomerase gene therapy in adult and old mice delays aging and increases longevity without increasing cancer. *EMBO molecular medicine* (2012).doi:10.1002/emmm.201200245
17. Lakatta, E. G. & Levy, D. Arterial and Cardiac Aging: Major Shareholders in Cardiovascular Disease Enterprises Part I: Aging Arteries: A ‘Set Up’ for Vascular Disease. *Circulation* **107**, 139–146 (2003).
18. Faller, A. & Schünke, M. *Der Körper des Menschen: Einführung in Bau und Funktion*. (Thieme, Stuttgart: 2008).
19. Ferrari, A. U., Radaelli, A. & Centola, M. Invited review: aging and the cardiovascular system. *J. Appl. Physiol.* **95**, 2591–2597 (2003).
20. Virmani, R., Avolio, A. P., Mergner, W. J., Robinowitz, M., Herderick, E. E., Cornhill, J. F., Guo, S. Y., Liu, T. H., Ou, D. Y. & O’Rourke, M. Effect of aging on aortic morphology in populations with high and low prevalence of hypertension and atherosclerosis. Comparison between occidental and Chinese communities. *Am J Pathol* **139**, 1119–1129 (1991).
21. Hampel, B., Fortschegger, K., Ressler, S., Chang, M. W., Unterluggauer, H., Breitwieser, A., Sommergruber, W., Fitzky, B., Lepperdinger, G., Jansen-Dürr, P., Voglauer, R. & Grillari, J. Increased expression of extracellular proteins as a hallmark of human endothelial cell in vitro senescence. *Exp. Gerontol.* **41**, 474–481 (2006).
22. Yildiz, O. Vascular smooth muscle and endothelial functions in aging. *Ann. N. Y. Acad. Sci.* **1100**, 353–360 (2007).
23. Donato, A. J., Eskurza, I., Silver, A. E., Levy, A. S., Pierce, G. L., Gates, P. E. & Seals, D. R. Direct evidence of endothelial oxidative stress with aging in humans: relation to impaired endothelium-dependent dilation and upregulation of nuclear factor-kappaB. *Circ. Res.* **100**, 1659–1666 (2007).
24. Fishbein, G. A. & Fishbein, M. C. Arteriosclerosis: rethinking the current classification. *Arch. Pathol. Lab. Med.* **133**, 1309–1316 (2009).
25. Lusis, A. J. Atherosclerosis. *Nature* **407**, 233–241 (2000).
26. Johnson, R. C., Leopold, J. A. & Loscalzo, J. Vascular calcification: pathobiological mechanisms and clinical implications. *Circ. Res.* **99**, 1044–1059 (2006).
27. Erusalimsky, J. D. & Kurz, D. J. Cellular senescence in vivo: its relevance in ageing and cardiovascular disease. *Exp. Gerontol.* **40**, 634–642 (2005).
28. Minamino, T., Miyauchi, H., Yoshida, T., Ishida, Y., Yoshida, H. & Komuro, I. Endothelial cell senescence in human atherosclerosis: role of telomere in endothelial dysfunction. *Circulation* **105**, 1541–1544 (2002).
29. Vasile, E., Tomita, Y., Brown, L. F., Kocher, O. & Dvorak, H. F. Differential expression of thymosin beta-10 by early passage and senescent vascular endothelium is modulated by VPF/VEGF: evidence for senescent endothelial cells in vivo at sites of atherosclerosis. *FASEB J.* **15**, 458–466 (2001).
30. Ogami, M., Ikura, Y., Ohsawa, M., Matsuo, T., Kayo, S., Yoshimi, N., Hai, E., Shirai, N., Ehara, S., Komatsu, R., Naruko, T. & Ueda, M. Telomere shortening in human coronary artery diseases. *Arterioscler. Thromb. Vasc. Biol.* **24**, 546–550 (2004).
31. Xu, D., Neville, R. & Finkel, T. Homocysteine accelerates endothelial cell senescence. *FEBS Lett.* **470**, 20–24 (2000).
32. Minamino, T. & Komuro, I. Vascular cell senescence: contribution to atherosclerosis. *Circ. Res.* **100**, 15–26 (2007).

33. Matthews, C., Gorenne, I., Scott, S., Figg, N., Kirkpatrick, P., Ritchie, A., Goddard, M. & Bennett, M. Vascular smooth muscle cells undergo telomere-based senescence in human atherosclerosis: effects of telomerase and oxidative stress. *Circ. Res.* **99**, 156–164 (2006).
34. Burton, D. G. A., Giles, P. J., Sheerin, A. N. P., Smith, S. K., Lawton, J. J., Ostler, E. L., Rhys-Williams, W., Kipling, D. & Faragher, R. G. A. Microarray analysis of senescent vascular smooth muscle cells: A link to atherosclerosis and vascular calcification. *Exp. Gerontol.* **44**, 659–665 (2009).
35. Nakano-Kurimoto, R., Ikeda, K., Uraoka, M., Nakagawa, Y., Yutaka, K., Koide, M., Takahashi, T., Matoba, S., Yamada, H., Okigaki, M. & Matsubara, H. Replicative senescence of vascular smooth muscle cells enhances the calcification through initiating the osteoblastic transition. *Am. J. Physiol. Heart Circ. Physiol.* **297**, H1673–1684 (2009).
36. Abedin, M., Tintut, Y. & Demer, L. L. Vascular calcification: mechanisms and clinical ramifications. *Arterioscler. Thromb. Vasc. Biol.* **24**, 1161–1170 (2004).
37. Ge, J., Chirillo, F., Schwedtmann, J., Gorge, G., Haude, M., Baumgart, D., Shah, V., von Birgelen, C., Sack, S., Boudoulas, H. & Erbel, R. Screening of ruptured plaques in patients with coronary artery disease by intravascular ultrasound. *Heart* **81**, 621–627 (1999).
38. Sage, A. P., Tintut, Y. & Demer, L. L. Regulatory Mechanisms in Atherosclerotic Calcification. *Nat Rev Cardiol* **7**, 528–536 (2010).
39. Long, F. Building strong bones: molecular regulation of the osteoblast lineage. *Nat. Rev. Mol. Cell Biol.* **13**, 27–38 (2012).
40. Burton, D. G. A., Matsubara, H. & Ikeda, K. Pathophysiology of vascular calcification: Pivotal role of cellular senescence in vascular smooth muscle cells. *Exp. Gerontol.* **45**, 819–824 (2010).
41. Komori, T., Yagi, H., Nomura, S., Yamaguchi, A., Sasaki, K., Deguchi, K., Shimizu, Y., Bronson, R. T., Gao, Y. H., Inada, M., Sato, M., Okamoto, R., Kitamura, Y., Yoshiki, S. & Kishimoto, T. Targeted disruption of *Cbfa1* results in a complete lack of bone formation owing to maturational arrest of osteoblasts. *Cell* **89**, 755–764 (1997).
42. Otto, F., Thornell, A. P., Crompton, T., Denzel, A., Gilmour, K. C., Rosewell, I. R., Stamp, G. W., Beddington, R. S., Mundlos, S., Olsen, B. R., Selby, P. B. & Owen, M. J. *Cbfa1*, a candidate gene for cleidocranial dysplasia syndrome, is essential for osteoblast differentiation and bone development. *Cell* **89**, 765–771 (1997).
43. Liu, W., Toyosawa, S., Furuichi, T., Kanatani, N., Yoshida, C., Liu, Y., Himeno, M., Narai, S., Yamaguchi, A. & Komori, T. Overexpression of *Cbfa1* in osteoblasts inhibits osteoblast maturation and causes osteopenia with multiple fractures. *J. Cell Biol.* **155**, 157–166 (2001).
44. Nakashima, K., Zhou, X., Kunkel, G., Zhang, Z., Deng, J. M., Behringer, R. R. & de Crombrughe, B. The novel zinc finger-containing transcription factor osterix is required for osteoblast differentiation and bone formation. *Cell* **108**, 17–29 (2002).
45. Zhou, X., Zhang, Z., Feng, J. Q., Dusevich, V. M., Sinha, K., Zhang, H., Darnay, B. G. & de Crombrughe, B. Multiple functions of Osterix are required for bone growth and homeostasis in postnatal mice. *Proc. Natl. Acad. Sci. U.S.A.* **107**, 12919–12924 (2010).
46. Wang, X., Kua, H.-Y., Hu, Y., Guo, K., Zeng, Q., Wu, Q., Ng, H.-H., Karsenty, G., de Crombrughe, B., Yeh, J. & Li, B. p53 functions as a negative regulator of osteoblastogenesis, osteoblast-dependent osteoclastogenesis, and bone remodeling. *J Cell Biol* **172**, 115–125 (2006).
47. Matsubara, T., Kida, K., Yamaguchi, A., Hata, K., Ichida, F., Meguro, H., Aburatani, H., Nishimura, R. & Yoneda, T. BMP2 Regulates Osterix through *Msx2* and *Runx2* during Osteoblast Differentiation. *J Biol Chem* **283**, 29119–29125 (2008).

48. Luo, G., Ducy, P., McKee, M. D., Pinero, G. J., Loyer, E., Behringer, R. R. & Karsenty, G. Spontaneous calcification of arteries and cartilage in mice lacking matrix GLA protein. *Nature* **386**, 78–81 (1997).
49. Murshed, M., Schinke, T., McKee, M. D. & Karsenty, G. Extracellular matrix mineralization is regulated locally; different roles of two gla-containing proteins. *J Cell Biol* **165**, 625–630 (2004).
50. Reynolds, J. L., Joannides, A. J., Skepper, J. N., McNair, R., Schurgers, L. J., Proudfoot, D., Jahnke-Dechent, W., Weissberg, P. L. & Shanahan, C. M. Human vascular smooth muscle cells undergo vesicle-mediated calcification in response to changes in extracellular calcium and phosphate concentrations: a potential mechanism for accelerated vascular calcification in ESRD. *J. Am. Soc. Nephrol.* **15**, 2857–2867 (2004).
51. Chen, N. X., Duan, D., O'Neill, K. D., Wolisi, G. O., Koczman, J. J., Laclair, R. & Moe, S. M. The mechanisms of uremic serum-induced expression of bone matrix proteins in bovine vascular smooth muscle cells. *Kidney Int.* **70**, 1046–1053 (2006).
52. Nakagawa, Y., Ikeda, K., Akakabe, Y., Koide, M., Uraoka, M., Yutaka, K.-T., Kurimoto-Nakano, R., Takahashi, T., Matoba, S., Yamada, H., Okigaki, M. & Matsubara, H. Paracrine osteogenic signals via bone morphogenetic protein-2 accelerate the atherosclerotic intimal calcification in vivo. *Arterioscler. Thromb. Vasc. Biol.* **30**, 1908–1915 (2010).
53. Byon, C. H., Javed, A., Dai, Q., Kappes, J. C., Clemens, T. L., Darley-Usmar, V. M., McDonald, J. M. & Chen, Y. Oxidative stress induces vascular calcification through modulation of the osteogenic transcription factor Runx2 by AKT signaling. *J. Biol. Chem.* **283**, 15319–15327 (2008).
54. Igarashi, M., Kamiya, N., Hasegawa, M., Kasuya, T., Takahashi, T. & Takagi, M. Inductive effects of dexamethasone on the gene expression of Cbfa1, Osterix and bone matrix proteins during differentiation of cultured primary rat osteoblasts. *J. Mol. Histol.* **35**, 3–10 (2004).
55. Huang, Y., Shen, X. J., Zou, Q. & Zhao, Q. L. Biological functions of microRNAs. *Bioorg. Khim.* **36**, 747–752 (2010).
56. Kapinas, K. & Delany, A. M. MicroRNA biogenesis and regulation of bone remodeling. *Arthritis Res. Ther.* **13**, 220 (2011).
57. van Rooij, E. The art of microRNA research. *Circ. Res.* **108**, 219–234 (2011).
58. Smith-Vikos, T. & Slack, F. J. MicroRNAs and their roles in aging. *J. Cell. Sci.* **125**, 7–17 (2012).
59. Hartmann, D. & Thum, T. MicroRNAs and vascular (dys)function. *Vascul. Pharmacol.* **55**, 92–105 (2011).
60. Valastyan, S., Reinhardt, F., Benaich, N., Calogrias, D., Szász, A. M., Wang, Z. C., Brock, J. E., Richardson, A. L. & Weinberg, R. A. A pleiotropically acting microRNA, miR-31, inhibits breast cancer metastasis. *Cell* **137**, 1032–1046 (2009).
61. Bhatnagar, N., Li, X., Padi, S. K. R., Zhang, Q., Tang, M.-S. & Guo, B. Downregulation of miR-205 and miR-31 confers resistance to chemotherapy-induced apoptosis in prostate cancer cells. *Cell Death Dis* **1**, e105 (2010).
62. Xi, S., Yang, M., Tao, Y., Xu, H., Shan, J., Inchauste, S., Zhang, M., Mercedes, L., Hong, J. A., Rao, M. & Schrupp, D. S. Cigarette smoke induces C/EBP- $\beta$ -mediated activation of miR-31 in normal human respiratory epithelia and lung cancer cells. *PLoS ONE* **5**, e13764 (2010).
63. Liu, C.-J., Lin, S.-C., Yang, C.-C., Cheng, H.-W. & Chang, K.-W. Exploiting salivary miR-31 as a clinical biomarker of oral squamous cell carcinoma. *Head Neck* **34**, 219–224 (2012).

64. Hua, D., Ding, D., Han, X., Zhang, W., Zhao, N., Foltz, G., Lan, Q., Huang, Q. & Lin, B. Human miR-31 targets radixin and inhibits migration and invasion of glioma cells. *Oncol. Rep.* **27**, 700–706 (2012).
65. Laurila, E. M., Sandström, S., Rantanen, L. M., Autio, R. & Kallioniemi, A. Both inhibition and enhanced expression of miR-31 lead to reduced migration and invasion of pancreatic cancer cells. *Genes Chromosomes Cancer* **51**, 557–568 (2012).
66. Rouas, R., Fayyad-Kazan, H., El Zein, N., Lewalle, P., Rothé, F., Simion, A., Akl, H., Mourtada, M., El Rifai, M., Burny, A., Romero, P., Martiat, P. & Badran, B. Human natural Treg microRNA signature: role of microRNA-31 and microRNA-21 in FOXP3 expression. *Eur. J. Immunol.* **39**, 1608–1618 (2009).
67. Sun, F., Wang, J., Pan, Q., Yu, Y., Zhang, Y., Wan, Y., Wang, J., Li, X. & Hong, A. Characterization of function and regulation of miR-24-1 and miR-31. *Biochem. Biophys. Res. Commun.* **380**, 660–665 (2009).
68. Mardaryev, A. N., Ahmed, M. I., Vlahov, N. V., Fessing, M. Y., Gill, J. H., Sharov, A. A. & Botchkareva, N. V. Micro-RNA-31 controls hair cycle-associated changes in gene expression programs of the skin and hair follicle. *FASEB J.* **24**, 3869–3881 (2010).
69. Staszal, T., Zapala, B., Polus, A., Sadakierska-Chudy, A., Kieć-Wilk, B., Stępień, E., Wybrańska, I., Chojnacka, M. & Dembińska-Kieć, A. Role of microRNAs in endothelial cell pathophysiology. *Pol. Arch. Med. Wewn.* **121**, 361–366 (2011).
70. Tang, Y.-F., Zhang, Y., Li, X.-Y., Li, C., Tian, W. & Liu, L. Expression of miR-31, miR-125b-5p, and miR-326 in the adipogenic differentiation process of adipose-derived stem cells. *OMICS* **13**, 331–336 (2009).
71. Zhang, Z., Zhang, H., Kang, Y., Sheng, P., Ma, Y., Yang, Z., Zhang, Z., Fu, M., He, A. & Liao, W. miRNA expression profile during osteogenic differentiation of human adipose-derived stem cells. *J. Cell. Biochem.* **113**, 888–898 (2012).
72. den Uyl, D., Bultink, I. E. M. & Lems, W. F. Advances in Glucocorticoid-Induced Osteoporosis. *Curr Rheumatol Rep* **13**, 233–240 (2011).
73. Patschan, D., Loddenkemper, K. & Buttgerit, F. Molecular mechanisms of glucocorticoid-induced osteoporosis. *Bone* **29**, 498–505 (2001).
74. Wang, C. C. L., Sorribas, V., Sharma, G., Levi, M. & Draznin, B. Insulin attenuates vascular smooth muscle calcification but increases vascular smooth muscle cell phosphate transport. *Atherosclerosis* **195**, e65–75 (2007).
75. Villa-Bellosta, R., Levi, M. & Sorribas, V. Vascular smooth muscle cell calcification and SLC20 inorganic phosphate transporters: effects of PDGF, TNF-alpha, and Pi. *Pflugers Arch.* **458**, 1151–1161 (2009).
76. Myers, M. A. Direct measurement of cell numbers in microtitre plate cultures using the fluorescent dye SYBR green I. *J. Immunol. Methods* **212**, 99–103 (1998).
77. Wada, T., McKee, M. D., Steitz, S. & Giachelli, C. M. Calcification of vascular smooth muscle cell cultures: inhibition by osteopontin. *Circ. Res.* **84**, 166–178 (1999).
78. Speer, M. Y., McKee, M. D., Guldberg, R. E., Liaw, L., Yang, H.-Y., Tung, E., Karsenty, G. & Giachelli, C. M. Inactivation of the Osteopontin Gene Enhances Vascular Calcification of Matrix Gla Protein-deficient Mice. *J Exp Med* **196**, 1047–1055 (2002).
79. Liu, X., Cheng, Y., Chen, X., Yang, J., Xu, L. & Zhang, C. MicroRNA-31 regulated by the extracellular regulated kinase is involved in vascular smooth muscle cell growth via large tumor suppressor homolog 2. *J. Biol. Chem.* **286**, 42371–42380 (2011).
80. Zhu, D., Mackenzie, N. C. W., Millán, J. L., Farquharson, C. & MacRae, V. E. The Appearance and Modulation of Osteocyte Marker Expression during Calcification of Vascular Smooth Muscle Cells. *PLoS One* **6**, (2011).
81. Luzi, E., Marini, F., Sala, S. C., Tognarini, I., Galli, G. & Brandi, M. L. Osteogenic differentiation of human adipose tissue-derived stem cells is modulated by the miR-26a targeting of the SMAD1 transcription factor. *J. Bone Miner. Res.* **23**, 287–295 (2008).



82. Hergenreider, E., Heydt, S., Tréguer, K., Boettger, T., Horrevoets, A. J. G., Zeiher, A. M., Scheffer, M. P., Frangakis, A. S., Yin, X., Mayr, M., Braun, T., Urbich, C., Boon, R. A. & Dimmeler, S. Atheroprotective communication between endothelial cells and smooth muscle cells through miRNAs. *Nat. Cell Biol.* **14**, 249–256 (2012).
83. Lee, K.-S., Kim, H.-J., Li, Q.-L., Chi, X.-Z., Ueta, C., Komori, T., Wozney, J. M., Kim, E.-G., Choi, J.-Y., Ryoo, H.-M. & Bae, S.-C. Runx2 Is a Common Target of Transforming Growth Factor  $\beta$ 1 and Bone Morphogenetic Protein 2, and Cooperation between Runx2 and Smad5 Induces Osteoblast-Specific Gene Expression in the Pluripotent Mesenchymal Precursor Cell Line C2C12. *Mol Cell Biol* **20**, 8783–8792 (2000).
84. Shruti, K., Shrey, K. & Vibha, R. Micro RNAs: tiny sequences with enormous potential. *Biochem. Biophys. Res. Commun.* **407**, 445–449 (2011).
85. Xu, J., Zhao, J., Evan, G., Xiao, C., Cheng, Y. & Xiao, J. Circulating microRNAs: novel biomarkers for cardiovascular diseases. *Journal of Molecular Medicine (Berlin, Germany)* (2011).doi:10.1007/s00109-011-0840-5
86. Thum, T. MicroRNA therapeutics in cardiovascular medicine. *EMBO Mol Med* **4**, 3–14 (2012).

## 10 Appendix

### 10.1 Zusammenfassung

Atherosklerose und Osteoporose sind zwei weitverbreitete, altersabhängige Krankheiten, die durch Kalziumablagerung, reguliert durch molekulare Mechanismen osteogener Differenzierung, gekennzeichnet sind. Vor kurzem entdeckten wir, dass seneszente Endothelzellen die osteogene Differenzierung von adipose-derived stem cells (Stammzellen, die aus Fettgewebe gewonnen werden) abschwächen können, indem sie Mikrovesikel sekretieren, welche mit einer microRNA, miR-31, angereichert sind. Von dieser Entdeckung ausgehend stellten wir zwei Hypothesen auf. Erstens, miR-31 inhibiert die Kalzifizierung von vaskulären glatten Muskelzellen (VSMCs) - ein Zelltyp, der in der Arteriosklerose osteogen zu differenzieren im Stande ist, was zur Kalzifizierung der Gefäße führt. Zweitens, Endothelzellen regulieren bei längerfristiger Behandlung mit Hydrocortison (HC) - ein Osteoporose verursachendes Glucocorticoid - miR-31 hoch. Wir beobachteten eine geringere Kalzifizierung in jenen VSMCs eines Spenders, die mit miR-31 transfeziert wurden. Bevor wir dieses Experiment beginnen konnten, testeten wir verschiedene Konzentrationen  $\text{Ca}^{2+}/\text{P}_i$  an VSMCs in Kultur aus. Des Weiteren adaptierten wir eine bereits etablierte Methode basierend auf der Färbung von Zellen mit SYBR Green I um die gewonnenen Daten auf den DNA-Gehalt normalisieren zu können. Zur Feststellung weiterer Targets von miR-31 entwarfen wir ein Luziferase-Reporter-Plasmid welches auf Grund zeitlicher Einschränkungen nicht zu Gänze fertiggestellt werden konnte. Um den Langzeiteffekt von Hydrocortison auf Endothelzellen zu untersuchen, inkubierten wir fünf Passagen lang humane Nabelschnurvenen-Endothelzellen (HUVECs) mit oder ohne HC und bestimmten die Expression von miR-31 mittels qPCR. In vorangegangenen kurzfristigen Experimenten stellten wir eine signifikante Hochregulierung von miR-31 fest. In dem vorliegenden längerfristigen Experiment jedoch gab es keine signifikanten Unterschiede in der Expression von miR-31 zwischen Zellen mit und solchen ohne HC im Medium.

## 10.2 Lebenslauf

### **Persönliche Daten**

Vor- und Zuname: Maximilian Bönisch

Geburtsdatum: 23. September 1984

Staatsbürgerschaft: Österreich

Eltern: Harald u. Helga Bönisch

Geschwister: eine Schwester

Familienstand: ledig

ohne religiöses Bekenntnis

### **Ausbildung**

1991 – 1995 Volksschule

1995 – 1999 Gymnasium Kundmannngasse

1999 – 2004 HAK I Vienna Business School

2004/2005 Absolvierung des Grundwehrdienstes

seit Oktober 2005 Studium der Biologie (Studienzweig Genetik/Mikrobiologie) an der Universität Wien

### **Praktika**

2007 zwei Monate bei Novartis Institutes for BioMedical Research

Dezember 2010 bis September 2011 bei Prof. Johannes Grillari zur Verfassung der Diplomarbeit

### **Auslandserfahrung**

Sommersemester 2010 Studium in Florenz, Italien, mit Erasmus-Stipendium

### **Sprachkenntnisse**

Deutsch (Muttersprache)

Englisch (fließend)

Italienisch (sehr gute Kenntnisse)

Französisch (Grundkenntnisse)

## 10.3 Vector maps

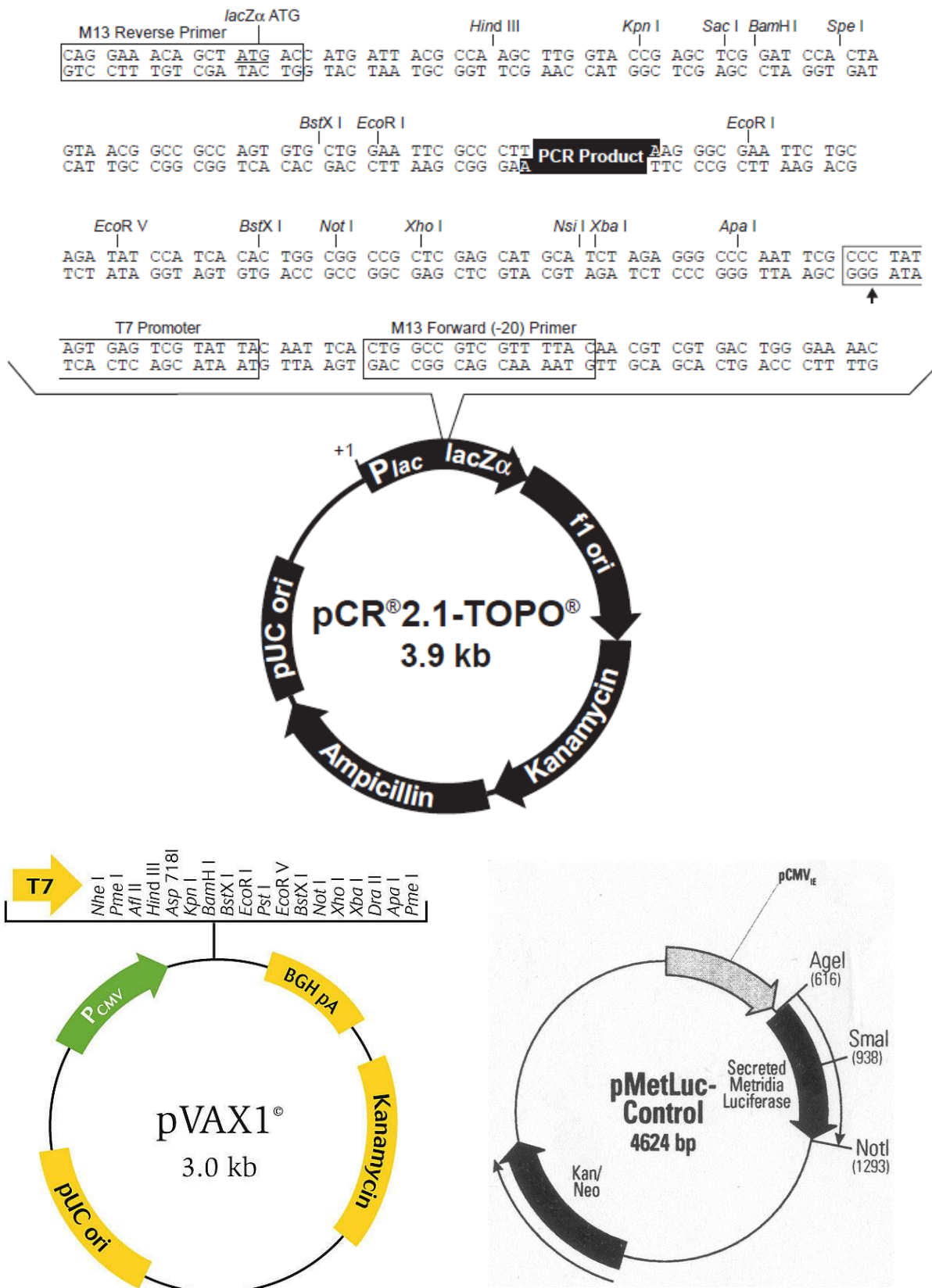


**Figure 38.** Vectors used to create the luciferase reporter plasmid. pCR2.1-TOPO (Invitrogen), pVAX1 (Invitrogen) and pMetLuc-Control (Clontech)

## 10.4 List of abbreviations

4-OHT .....	4-hydroxytamoxifen
ALP .....	alkaline phosphatase
antis. ....	antisense
AoSMCs .....	aortic smooth muscle cells
ASCs.....	adipose-derived stem cells
BGLAP.....	bone gamma-carboxyglutamic acid-containing protein (osteocalcin)
BMP .....	bone morphogenetic protein
C. elegans .....	Caenorhabditis elegans
ctr#2.....	control#2
CVD .....	cardiovascular disease
DDR .....	DNA damage response
DGCR8.....	DiGeorge syndrome critical region gene 8
Dkk-1.....	Dickkopf-1
DMEM .....	Dulbecco's Modified Eagle's Medium
eIF.....	eukaryotic initiation factor
FBS .....	foetal bovine serum
FGF.....	fibroblast growth factor
FI .....	fluorescence intensity
FOXP3.....	forkhead box P3
Fzd.....	frizzled
GAPDH .....	glyceraldehyde 3-phosphate dehydrogenase
GC .....	glucocorticoid
HC .....	hydrocortisone
hPLALP.....	human placental alkaline phosphatase
HUVECs.....	human umbilical vein endothelial cells
MGP .....	matrix Gla protein
miRNA/miR ....	microRNA
NFW .....	nuclease free water
PD.....	population doubling

PP<sub>i</sub>..... inorganic pyrophosphate  
 pre-miRNA..... precursor microRNA  
 pri-miRNA ..... primary microRNA  
 qPCR ..... quantitative polymerase chain reaction  
 RISC ..... RNA-induced silencing complex  
 ROS ..... reactive oxygen species  
 RT..... reverse transcriptase  
 Runx2 ..... Runt-related transcription factor 2  
 SASP ..... senescence-associated secretory phenotype  
 SA-β-gal ..... senescence-associated β-galactosidase  
 SDS..... sodium dodecyl sulphate  
 SIPS ..... stress-induced premature senescence  
 SPP1 ..... secreted phosphoprotein 1 (osteopontin)  
 TERT ..... telomerase reverse transcriptase  
 TGF-β ..... transforming growth factor-β  
 transf..... transfected  
 TRBP..... TAR RNA binding protein  
 UTR..... untranslated region  
 VSMCs ..... vascular smooth muscle cells\*